4722 *Inorg. Chem.* **1995**, *34*, 4722−4734

Carbonyl Derivatives of Chloride−Dimethyl Sulfoxide−Ruthenium(II) Complexes: Synthesis, Structural Characterization, and Reactivity of $\mathrm{Ru(CO)}_x\mathrm{(DMSO)}_{4-x}\mathrm{Cl_2}$ Complexes (x = 1−3)

E. Alessio,*,† B. Milani,† M. Bolle,† G. Mestroni,† P. Faleschini,† F. Todone,† S. Geremia,‡ and M. Calligaris*,†

Dipartimento di Scienze Chimiche, Università di Trieste, Via L. Giorgieri 1, 34127 Trieste, Italy, and Dipartimento di Scienze dei Materiali e della Terra, Università di Ancona, Via delle Brecce Bianche, Ancona, Italy

Received December 22, 1994[⊗]

The reactivity of *cis*- and *trans*-RuCl$_2$(DM*S*O)$_4$ with carbon monoxide has been thoroughly investigated. Depending on the choice of the solvent and the reaction conditions, *cis*-RuCl$_2$(DMSO)$_4$ reacts with CO at ambient pressure replacing one, two or three DMSO molecules. The following derivatives have been isolated: *trans,cis,cis*-Ru(CO)(DMS*O*)(DM*S*O)$_2$Cl$_2$ (**1**), *cis,cis,cis*-Ru(CO)$_2$(DM*S*O)(DMS*O*)Cl$_2$ (**2**), *cis,trans,cis*-Ru(CO)$_2$(DM*S*O)$_2$Cl$_2$ (**3**) and *fac*-Ru(CO)$_3$(DMS*O*)Cl$_2$ (**4**). Compounds **1**, **3** and **4** have been structurally characterized. **1**·0.5H$_2$O: monoclinic, $P2_1/c$, $Z = 8$, $a = 15.408(1)$ Å, $b = 15.398(2)$ Å, $c = 14.826(1)$ Å, $\beta = 107.46(1)°$. **3**: orthorhombic, $Pca2_1$, $Z = 8$, $a = 15.853(3)$ Å, $b = 11.380(2)$ Å, $c = 14.874(2)$ Å. **4**: orthorhombic, $P2_12_12_1$, $Z = 4$, $a = 7.300(2)$ Å, $b = 9.297(2)$ Å, $c = 16.515(4)$ Å, $\beta = 107.46(1)°$. Reaction of *trans*-RuCl$_2$(DM*S*O)$_4$ with CO at room temperature and ambient pressure leads to the replacement of either one or two DMSO ligands, depending on the reaction time, yielding *trans,trans,trans*-Ru(CO)(DMS*O*)(DM*S*O)$_2$Cl$_2$ (**5**) and *cis,cis,trans*-Ru(CO)$_2$(DMS*O*)$_2$Cl$_2$ (**6**). The crystal structure of **5** has been determined. **5**: monoclinic, $P2_1$, $Z = 4$, $a = 7.417(3)$ Å, $b = 26.808(6)$ Å, $c = 8.368(4)$ Å, $\beta = 107.55(7)°$. Complex **3** is the thermodynamically most stable bis(carbonyl) species. Compounds **1**−**6** represent the first example of well-characterized Ru(II) chloride−DMSO−carbonyl complexes. Their most striking common feature is that coordination of carbon monoxide induces the selective isomerization of the DMSO trans to it from S- to O-bonding. Compounds **1**−**6** are versatile precursors for the synthesis of carbonylated Ru(II) species in which the DMSO ligands are partially or completely replaced by other ligands. Reaction of **1**−**6** with pyridine has been investigated and several products were isolated. The reactions were often accompanied by a geometrical isomerization. Complex **1** yields *cis,cis,cis*-Ru(CO)(py)(DM*S*O)$_2$Cl$_2$ (**7**), whose crystal structure has been determined. **7**: triclinic, $P\bar{1}$, $Z = 2$, $a = 7.129(3)$ Å, $b = 7.918(2)$ Å, $c = 14.516(7)$ Å, $\alpha = 84.70(3)°$, $\beta = 88.14(3)°$, $\gamma = 77.87(3)°$. Complex **3** can replace either one DMSO ligand, forming the two geometrical isomers *cis,cis,cis*-Ru(CO)$_2$(py)(DM*S*O)Cl$_2$ (**8**) and *cis,trans,cis*-Ru(CO)$_2$(py)(DM*S*O)Cl$_2$ (**9**), or two DMSO ligands, yielding *cis,cis,trans*-Ru(CO)$_2$(py)$_2$Cl$_2$ (**10**), where a *cis* to *trans* isomerization of the two chlorides occurred. Also the crystal structure of **9** has been determined; **9**: triclinic, $P\bar{1}$, $Z = 4$, $a = 7.939(3)$ Å, $b = 12.863(5)$ Å, $c = 14.133(3)$ Å, $\alpha = 105.95(2)°$, $\beta = 95.10(2)°$, $\gamma = 99.02(2)°$. *fac*-Ru(CO)$_3$(py)Cl$_2$ (**11**) was obtained from **4**, while *cis,cis,trans*-Ru(CO)(DM*S*O)(py)$_2$Cl$_2$ (**12**) and *cis,cis,trans*-Ru(CO)$_2$(py)$_2$Cl$_2$ (**10**) were synthesized from **5** and **6**, respectively.

Introduction

A wide series of halocarbonyl−ruthenium(II) complexes with neutral ligands of general formula Ru(CO)L$_3$X$_2$, Ru(CO)$_2$L$_2$X$_2$, and Ru(CO)$_3$LX$_2$, with X = Cl, Br, and I and L = P, N, As, and S donor ligands, is known in the literature.[1] Such complexes have been prepared either by substitution reactions starting from carbonyl species or by carbonylation reactions of suitable precursors already bearing the L ligands. Each stoichiometry can provide, in principle, a number of geometrical isomers. The designations refer, in order, to the arrangements of CO, L, and X.[1]

Despite the quite extensive studies done in this field, in particular when L = phosphine ligand,[2−5] and despite the fact that Ru(II)−DMSO complexes are well-known precursors in the synthesis of Ru(II) compounds, only one example of a chlorocarbonylruthenium(II) complex with DMSO was known to date. The product, of formula Ru(CO)$_2$(DMSO)$_2$Cl$_2$, was obtained by Evans et al.[6] upon carbonylation of *cis*-RuCl$_2$(DMSO)$_4$ and reported without details on its geometry or the binding mode of the two sulfoxide molecules. A bis(carbonyl) complex with O-bonded methyl 2-methylbutyl sulfoxide (MBMSO), tentatively formulated as *cis,trans,cis*-Ru(CO)$_2$(MBMSO)$_2$Cl$_2$, has also been described.[7] A few examples of monocarbonyl mixed-ligand complexes with one DMSO and two phosphine ligands have been reported.[4,8]

As a natural extension of our studies on carbonylated derivates of chloro−dimethyl sulfoxide−ruthenium(III) complexes[9] and of our interest in the chemistry of Ru(II) compounds,[10−14] we

---

† Università di Trieste.

‡ Università di Ancona.

⊗ Abstract published in *Advance ACS Abstracts*, August 1, 1995.

(1) Seddon, E. A.; Seddon, K. R. In *The Chemistry of Ruthenium*; Clark, R. J. H., Ed.; Elsevier: Amsterdam, The Netherlands, 1984.

(2) Jenkins, J. M.; Lupin, M. S.; Shaw, B. L. *J. Chem. Soc. A* **1966**, 1787.

(3) Colton, R.; Farthing, R. H. *Aust. J. Chem.* **1967**, *20*, 1283.

(4) Barnard, C. F. J.; Daniels, J. A.; Jeffrey, J.; Mawby, R. J. *J. Chem. Soc., Dalton Trans.* **1976**, 953.

(5) Barnard, C. F. J.; Daniels, J. A.; Jeffrey, J.; Mawby, R. J. *J. Chem. Soc., Dalton Trans.* **1976**, 1861.

(6) Evans, I. P.; Spencer, A.; Wilkinson, G. *J. Chem. Soc., Dalton Trans.* **1973**, 204.

(7) McMillan, R. S. Ph.D. Thesis, University of British Columbia, Vancouver, Canada, 1976.

(8) James, B. R.; Markham, L. D.; Hui, B. C.; Rempel, G. L. *J. Chem. Soc., Dalton Trans.* **1973**, 2247.

0020-1669/95/1334-4722$09.00/0 © 1995 American Chemical Society

Table 1. Crystallographic Data for **1**, **3**, **4**, **5**, **7**, and **9**

	1	**3**	**4**	**5**	**7**	**9**
formula	$C_7H_{18}Cl_2O_4RuS_3{\cdot}0.5H_2O$	$C_6H_{12}Cl_2O_4RuS_2$	$C_5H_6Cl_2O_4RuS$	$C_7H_{18}Cl_2O_4RuS_3$	$C_{10}H_{17}Cl_2NO_3RuS_2$	$C_9H_{11}Cl_2NO_3RuS$
M_r	443.4	384.4	334.1	434.4	435.4	385.2
cryst syst	monoclinic	orthorhombic	orthorhombic	monoclinic	triclinic	triclinic
space group	$P2_1/c$	$Pca2_1$	$P2_12_12_1$	$P2_1$	$P\bar{1}$	$P\bar{1}$
a, Å	15.408(1)	15.853(3)	7.300(2)	7.417(3)	7.129(3)	7.939(3)
b, Å	15.398(2)	11.380(2)	9.297(2)	26.808(6)	7.918(2)	12.863(5)
c, Å	14.826(1)	14.874(2)	16.515(4)	8.368(4)	14.516(7)	14.133(3)
α, deg	90	90	90	90	84.70(3)	105.95(2)
β, deg	107.46(1)	90	90	107.55(7)	88.14(3)	95.10(2)
γ, deg	90	90	90	90	77.87(3)	99.02(2)
V, Å^3	3355(1)	2683(1)	1120.8(8)	1586(2)	797.5(8)	1357(2)
Z	8	8	4	4	2	4
ϱ_{calc}, g cm^{-3}	1.76	1.90	1.98	1.82	1.81	1.89
radiation	Mo Kα graphite-monochromated, $\lambda = 0.7107$ Å					
μ (Mo Kα), cm^{-1}	16.0	18.4	20.1	16.9	15.6	16.7
scan type	ω	$\omega-2\theta$	ω	$\omega-2\theta$	$\omega-2\theta$	$\omega-2\theta$
θ range, deg	2−26	2−30	2−30	2−30	2−28	2−30
no. of intens monitored[a]	3	3	3	3	3	3
no. of unique data with $I > 3\sigma(I)$	4277	3326	1545	2930	3301	6718
data/param ratio	13.2	12.3	13.0	9.6	19.1	21.8
w	$1/[1 + \sigma(F_o)^2 + (0.02\lvert F_o\rvert)^2]$	$4F_o^2/[\sigma(I) + (0.04F_o^2)^2]$	1	$4F_o^2/[\sigma(I) + (0.04F_o)^2]$	1	1
R[b]	0.036	0.026	0.027	0.045	0.022	0.027
R_w[c]	0.039	0.030	0.026	0.054	0.021	0.034
GOF[d]	0.40	0.91	0.88	1.62	0.58	1.03

[a] Measured after each 5000 s. [b] $R = \sum\lvert\lvert F_o\rvert - \lvert F_c\rvert\rvert/\sum\lvert F_o\rvert$. [c] $R_w = \sum[w(\lvert F_o\rvert - \lvert F_c\rvert)^2/\sum w\lvert F_o\rvert^2]^{1/2}$. [d] GOF = $[\sum w(\lvert F_o\rvert - \lvert F_c\rvert)^2/(m - n)]^{1/2}$; m = no. of observations; n = no. of variables.

report here a series of new, fully characterized chlorocarbonylruthenium(II) complexes with DMSO, obtained upon carbonylation of *cis* and *trans*-$RuCl_2(DMSO)_4$. Compared to the known examples with other neutral ligands, in this case the number of possible isomers is increased by the ability of DMSO to bind either through sulfur (DM*S*O) or through oxygen (DMS*O*) to the Ru(II) center.

The reactivity of the new compounds toward pyridine (py) has also been investigated. Several derivatives, obtained upon substitution of DMSO ligands with py, are described here. In no case was substitution of CO observed.

Experimental Section

Solid state infrared spectra were obtained as Nujol mulls between CsI windows on a Perkin-Elmer 983G spectrometer. Chloroform spectra in the CO stretching region were recorded between NaCl windows (0.1 mm spacer). ^{1}H and ^{13}C NMR spectra were recorded at 400 and 100.5 MHz, respectively, on a JEOL EX400 FT instrument. All spectra were run at room temperature and referenced to TMS. A pulse delay of 10 s was applied in ^{13}C spectra to allow for relaxation of carbonylic carbon atoms. 2D COSY spectra were recorded using the built-in automatic program of the Jeol instrument. The following conditions were used for the NOESY spectrum: matrix of 512 × 1024 data points; the second dimension was zero filled to 1024 data points prior to Fourier transformation; 16 scans per t_1 increment were preceded by two dummy scans, with a spectral window of 3203 Hz, pulse delay of 2.34 s, a mixing time of 500 ms, and a square sine bell function with no phase shift applied in both dimensions. Data were processed with the computer of the instrument. Unless otherwise stated, spectra were recorded immediately after dissolution of the complexes. Elemental analyses were performed by Dr. E. Cebulec (Dipartimento Scienze Chimiche, Università di Trieste).

Synthesis of the Complexes. *cis*- and *trans*-$RuCl_2(DMSO)_4$ were synthesized according to the published procedure.[10]

***trans,cis,cis*-Ru(CO)(DM*S*O)(DMS*O*)$_2$Cl$_2$ (1).** A 1 g amount of *cis*-$RuCl_2(DMSO)_4$ (2 mmol) was partially dissolved in 60 mL of methanol in a flask closed with a stopcock. The flask was first connected to a vacuum line and then to a reservoir of CO. Within 1.5 h the starting material dissolved completely and a clear pale yellow solution was obtained. After an additional hour of reaction, the solution was concentrated to 5 mL and stored at 4 °C after addition of some diethyl ether. Yellow crystals of the product formed in a few hours from the solution. They were filtered off, washed with cold methanol and diethyl ether, and vacuum dried. Yield: 0.54 g (60%). Anal. Calcd for $C_7H_{18}Cl_2O_4RuS_3$ (M_r = 434.37): C, 19.35; H, 4.17; S, 22.14. Found: C, 19.2; H, 4.05; S, 22.2. UV/visible spectra (λ_{max}, nm (ϵ, M^{-1} cm^{-1})): in CHCl$_3$ solution, 370 (161), 311 (670). Selected IR absorption bands: Nujol, ν_{CO} 1995 cm^{-1} (vs), ν_{SO} 1134 (vs) (DM*S*O), 924 cm^{-1} (s) (DMS*O*), ν_{Ru-C} 517 cm^{-1} (w), ν_{Ru-O} 472 cm^{-1} (m), ν_{Ru-S} 422 cm^{-1} (m), ν_{Ru-Cl} 332, 296 cm^{-1} (m); CHCl$_3$ solution, ν_{CO} 2007 cm^{-1} (vs). ^{1}H NMR spectrum in CDCl$_3$: 3.43 (s, 6, DM*S*O), 3.26 (s, 6, DM*S*O), 2.85 ppm (s, 6, DMS*O*). ^{13}C NMR spectrum in CDCl$_3$: 196.0 (1, CO), 47.6 (2, DM*S*O), 46.7 (2, DM*S*O), 39.1 (2, DMS*O*).

***cis,cis,cis*-Ru(CO)$_2$(DM*S*O)(DMS*O*)Cl$_2$ (2).** A 0.3 g amount of *cis*-$RuCl_2(DMSO)_4$ (0.62 mmol) was partially dissolved in 24 mL of methanol and reacted with CO at room temperature for 42 h. The clear, almost colorless solution obtained was concentrated to 8 mL and stored at 4 °C after addition of some diethyl ether. A white precipitate of the product slowly formed over 48 h and was then filtered, washed with cold methanol and diethyl ether, and vacuum dried. Yield: 0.08 g (35%). Anal. Calcd for $C_6H_{12}Cl_2O_4RuS_2$ (M_r = 384.25): C, 18.75; H, 3.14; S, 16.68. Found: C, 18.5; H, 3.08; S, 16.4. UV/visible spectra (λ_{max}, nm (ϵ, M^{-1} cm^{-1})): in CHCl$_3$ solution, 307.5 (sh, 814). Selected IR absorption bands: Nujol, ν_{CO} 2077, 2018 cm^{-1} (vs), ν_{SO} 1131 (vs) (DM*S*O), ν_{SO} 926 (vs) (DMS*O*), ν_{Ru-O} 473 cm^{-1} (m), ν_{Ru-S} 422 cm^{-1} (m), ν_{Ru-Cl} 326, 294 cm^{-1} (m); CHCl$_3$ solution, ν_{CO} 2083, 2023 cm^{-1} (vs). ^{1}H NMR spectrum in CDCl$_3$: 3.42 (s, 3, DM*S*O), 3.17 (s, 3, DM*S*O), 2.89 (s, 3, DMS*O*), 2.86 ppm (s, 3, DMS*O*). ^{13}C NMR spectrum in CDCl$_3$: 191.9 (1, CO), 186.1 (1, CO), 47.4 (1, DM*S*O), 42.3 (1, DM*S*O), 39.2 (1, DMS*O*), 38.9 ppm (1, DMS*O*).

---

(9) Alessio, E.; Bolle, M.; Milani, B.; Mestroni, G.; Faleschini, P.; Geremia S.; Calligaris, M. *Inorg. Chem.* **1995**, *34*, 4716.

(10) Alessio, E.; Mestroni, G.; Nardin, G.; Attia, W. M.; Calligaris, M.; Sava, G.; Zorzet, S. *Inorg. Chem.* **1988**, *27*, 4099.

(11) Alessio, E.; Milani, B.; Mestroni, G.; Calligaris, M.; Faleschini, P.; Attia, W. M. *Inorg. Chim. Acta* **1990**, *177*, 255.

(12) Henn, M.; Alessio, E.; Mestroni, G.; Calligaris, M.; Attia, W. M. *Inorg. Chim. Acta* **1991**, *187*, 39.

(13) Alessio, E.; Milani, B.; Calligaris, M.; Bresciani-Pahor, N. *Inorg. Chim. Acta* **1992**, *194*, 85.

(14) Marzilli, L. G.; Iwamoto, M.; Alessio, E.; Hansen, L.; Calligaris, M. *J. Am. Chem. Soc.* **1994**, *116*, 815.

Table 2. Positional Parameters and *B* Values with Estimated Standard Deviations for **1**

atom	*x*	*y*	*z*	B_{eq},[a] Å^2
		Molecule **A**		
Ru1	0.80587(3)	0.20574(3)	0.13412(3)	2.690(9)
Cl1A	0.7301(1)	0.3213(1)	0.0323(1)	4.29(4)
Cl2A	0.6717(1)	0.1184(1)	0.0662(1)	4.15(4)
S1A	0.9276(1)	0.2954(1)	0.1921(1)	3.35(3)
S2A	0.8727(1)	0.0978(1)	0.2388(1)	3.41(3)
S3A	0.6455(1)	0.2725(1)	0.2170(1)	3.97(4)
O1A	1.0131(3)	0.2543(4)	0.2474(4)	5.1(1)
O2A	0.9463(3)	0.0488(4)	0.2197(4)	5.3(1)
O3A	0.7474(3)	0.2493(3)	0.2400(3)	3.8(1)
O4A	0.8786(3)	0.1294(4)	−0.0124(3)	5.4(1)
C1A	0.9014(5)	0.3796(5)	0.2605(6)	5.6(2)
C2A	0.9538(5)	0.3579(5)	0.1034(5)	4.5(2)
C3A	0.7921(6)	0.0218(5)	0.2523(6)	5.5(2)
C4A	0.9108(5)	0.1353(5)	0.3575(5)	4.7(2)
C5A	0.5995(5)	0.1894(7)	0.2702(6)	6.0(2)
C6A	0.6479(6)	0.3568(7)	0.2993(7)	7.5(2)
C7A	0.8532(4)	0.1603(5)	0.0443(4)	3.4(1)
		Molecule B		
Ru2	0.27032(3)	0.25650(4)	0.10789(3)	3.02(1)
Cl1B	0.3426(1)	0.1308(1)	0.1948(1)	5.17(5)
Cl2B	0.4064(1)	0.3383(1)	0.1832(1)	4.91(4)
S1B	0.1453(1)	0.1730(1)	0.0416(1)	3.35(3)
S2B	0.2060(1)	0.3752(1)	0.0181(1)	3.44(3)
S3B	0.4284(1)	0.1969(1)	0.0212(1)	3.89(4)
O1B	0.0626(3)	0.2174(3)	−0.0132(3)	4.6(1)
O2B	0.1298(3)	0.4175(4)	0.0402(3)	4.9(1)
O3B	0.3273(3)	0.2229(3)	−0.0020(3)	4.0(1)
O4B	0.2034(4)	0.3139(4)	0.2667(3)	5.2(1)
C1B	0.1158(5)	0.1076(5)	0.1265(5)	5.1(2)
C2B	0.1707(5)	0.0914(5)	−0.0313(5)	5.0(2)
C3B	0.1726(6)	0.3515(5)	−0.1049(5)	5.1(2)
C4B	0.2861(5)	0.4563(5)	0.0188(7)	5.7(2)
C5B	0.4259(6)	0.1025(7)	−0.0454(9)	9.0(3)
C6B	0.4722(6)	0.2685(8)	−0.0456(7)	7.9(3)
C7B	0.2259(4)	0.2911(4)	0.2042(4)	3.6(1)
O5	0.4790(7)	0.010(1)	0.4358(8)	9.3(4)
O6	0.560(1)	−0.0121(8)	0.6240(8)	8.4(4)

[a] Values for anisotropically refined atoms are given in the from of the isotropic equivalent displacement parameter defined as $B_{eq} = (4/3)[a^2\beta(1,1) + b^2\beta(2,2) + c^2\beta(3,3) + ab(\cos\gamma)\beta(1,2) + ac(\cos\beta)\beta(1,3) + bc(\cos\alpha)\beta(2,3)]$.

Table 3. Positional Parameters and *B* Values with Estimated Standard Deviations for **3**

atom	*x*	*y*	*z*	B_{eq},[a] Å^2
RuA	0.13509(2)	0.02384(3)	0.500	2.111(5)
Cl1A	0.17772(9)	0.2039(1)	0.4305(1)	3.82(3)
Cl2A	0.02413(8)	0.1228(2)	0.5798(1)	4.26(3)
S1A	0.22928(7)	0.0597(1)	0.62011(8)	2.53(2)
S2A	0.03165(8)	−0.0070(1)	0.38893(9)	2.82(2)
O1A	0.2740(2)	−0.0888(4)	0.3907(3)	4.69(9)
O2A	0.0862(4)	−0.2041(4)	0.5882(4)	6.8(1)
O11A	0.2380(3)	−0.0375(3)	0.6842(3)	3.82(8)
O21A	−0.0362(3)	−0.0870(4)	0.4145(3)	4.63(9)
C1A	0.2223(3)	−0.0467(5)	0.4329(4)	3.00(9)
C12A	0.2032(4)	0.1885(6)	0.6810(5)	4.9(1)
C11A	0.3305(4)	0.0994(6)	0.5783(5)	4.4(1)
C2A	0.1039(4)	−0.1189(5)	0.5556(4)	3.9(1)
C21A	−0.0140(4)	0.1262(6)	0.3510(5)	4.9(1)
C22A	0.0786(4)	−0.0599(7)	0.2892(4)	4.9(1)
RuB	0.12152(2)	0.55685(3)	0.14025(3)	1.946(5)
Cl1B	0.24797(8)	0.4722(1)	0.08092(9)	3.41(2)
Cl2B	0.07559(9)	0.3700(1)	0.1983(1)	3.75(3)
S1B	0.05824(6)	0.5143(1)	0.00055(9)	2.54(2)
S2B	0.19394(8)	0.5959(1)	0.27520(8)	2.58(2)
O1B	−0.0379(3)	0.6453(4)	0.2274(3)	5.02(9)
O2B	0.1794(3)	0.7844(4)	0.0585(3)	4.9(1)
O11B	0.0885(3)	0.5887(4)	−0.0729(3)	3.89(8)
O21B	0.1442(3)	0.6579(4)	0.3444(3)	4.14(9)
C1B	0.0217(3)	0.6163(5)	0.1925(4)	3.2(1)
C2B	0.1566(3)	0.7012(4)	0.0906(3)	2.82(9)
C11B	−0.0528(3)	0.5245(7)	0.0067(5)	4.9(1)
C12B	0.0716(4)	0.3655(6)	−0.0310(4)	3.9(1)
C21B	0.2375(4)	0.4657(5)	0.3233(4)	3.8(1)
C22B	0.2884(4)	0.6757(5)	0.2554(4)	3.7(1)

[a] Values for anisotropically refined atoms are given in the from of the isotropic equivalent displacement parameter defined as $(4/3)[a^2\beta(1,1) + b^2\beta(2,2) + c^2\beta(3,3) + ab(\cos\gamma)\beta(1,2) + ac(\cos\beta)\beta(1,3) + bc(\cos\alpha)\beta(2,3)]$.

Table 4. Positional Parameters and *B* Values with Estimated Standard Deviations for **4**

atom	*x*	*y*	*z*	B_{eq},[a] Å^2
Ru	0.88738(6)	0.56965(4)	0.65927(2)	3.327(6)
Cl1	0.9446(2)	0.6185(2)	0.51997(9)	4.61(3)
Cl2	1.0091(2)	0.3310(1)	0.64359(9)	4.14(3)
S	0.6074(2)	0.3902(1)	0.55445(8)	3.76(2)
O1	0.8050(7)	0.4938(5)	0.8331(3)	6.6(1)
O2	0.7211(7)	0.8668(4)	0.6710(3)	6.8(1)
O3	1.2685(6)	0.6719(5)	0.6995(3)	6.4(1)
O4	0.6292(5)	0.4876(4)	0.6289(2)	4.32(7)
C1	0.8336(9)	0.5240(6)	0.7684(3)	4.4(1)
C2	0.7820(8)	0.7572(6)	0.6677(4)	4.2(1)
C3	1.1222(9)	0.6373(6)	0.6860(3)	4.5(1)
C4	0.4217(9)	0.4689(7)	0.5025(4)	5.1(1)
C5	0.4992(9)	0.2348(7)	0.5942(4)	5.0(1)

[a] Values for anisotropically refined atoms are given in the from of the isotropic equivalent displacement parameter defined as $(4/3)[a^2\beta(1,1) + b^2\beta(2,2) + c^2\beta(3,3) + ab(\cos\gamma)\beta(1,2) + ac(\cos\beta)\beta(1,3) + bc(\cos\alpha)\beta(2,3)]$.

The procedure is however scarcely reproducible and the product is often contaminated by variable amounts of **1** and **3**.

***cis*,*trans*,*cis*-Ru(CO)$_2$(DMSO)$_2$Cl$_2$ (3).** A procedure very similar to that reported in the literature[6] was adopted. A 1 g amount of *cis*-RuCl$_2$(DMSO)$_4$ (2 mmol) was heated to reflux in 200 mL of toluene under a stream of CO for 8 h. The resulting colorless solution was concentrated to 150 mL and stored at room temperature. Needle-shaped crystals of the product formed within 3 days and were then filtered, washed with diethyl ether, and vacuum dried. Yield: 0.40 g (50%). Anal. Calcd for C$_6$H$_{12}$Cl$_2$O$_4$RuS$_2$ (M_r = 384.25): C, 18.75; H, 3.14; S, 16.68. Found: C, 18.8; H, 3.14; S, 16.5. UV/visible spectra (λ_{max}, nm (ϵ, M^{-1} cm^{-1})): in CHCl$_3$ solution, 308 (sh, 1297), 300 (1545), 257 (13 000). Selected IR absorption bands: Nujol, ν_{CO} 2089, 2035 cm^{-1} (vs), ν_{SO} 1129 (vs) (DM*S*O), ν_{Ru-C} 484 cm^{-1} (m), ν_{Ru-S} 412 cm^{-1} (m), ν_{Ru-Cl} 328, 311 cm^{-1} (m); CHCl$_3$ solution, ν_{CO} 2093, 2038 cm^{-1} (vs). ^{1}H NMR spectrum in CDCl$_3$: 3.44 ppm (s, 12, DM*S*O). ^{13}C NMR spectrum in CDCl$_3$: 185.0 (2, CO), 45.1 (4, DMSO).

***fac*-Ru(CO)$_3$(DMS*O*)Cl$_2$ (4).** A 0.5 g amount of *cis*-RuCl$_2$(DMSO)$_4$ (1 mmol) was heated to reflux in 40 mL of absolute ethanol under a stream of CO for 3 h. The resulting pale yellow solution was concentrated to 10 mL and stored at 4 °C after addition of some diethyl ether. Needle-shaped crystals of the product formed overnight and were then filtered, washed with cold ethanol and diethyl ether, and vacuum dried. Yield: 0.23 g (70%). Anal. Calcd for C$_5$H$_6$Cl$_2$O$_4$RuS (M_r = 334.13): C, 17.97; H, 1.81; S, 9.59. Found: C, 18.1; H, 1.78; S, 9.63. UV/visible spectra (λ_{max}, nm (ϵ, M^{-1} cm^{-1})): in CHCl$_3$ solution, 290 (1575). Selected IR absorption bands: Nujol, ν_{CO} 2129, 2060 cm^{-1} (vs), ν_{SO} 933 (vs) (DMS*O*), ν_{Ru-O} 470 cm^{-1} (m), ν_{Ru-Cl} 325, 296 cm^{-1} (m); CHCl$_3$ solution, ν_{CO} 2134, 2063 cm^{-1} (vs). ^{1}H NMR spectrum in CDCl$_3$: 2.83 ppm (s, 6, DMS*O*). ^{13}C NMR spectrum in CDCl$_3$: 187.0 (1, CO), 183.0 (2, CO), 39.1 (2, DMS*O*).

***trans*,*trans*,*trans*-Ru(CO)(DMS*O*)(DMSO)$_2$Cl$_2$ (5).** A 0.3 g amount of *trans*-RuCl$_2$(DMSO)$_4$ (0.62 mmol) was partially dissolved in 18 mL of methanol and reacted with CO for 45 min. The clear, deep-yellow solution obtained was concentrated to 2 mL and stored at 4 °C after addition of some diethyl ether. Needle-shaped yellow crystals of the product formed overnight and were then filtered, rapidly washed with cold methanol and diethyl ether, and vacuum dried. Yield: 0.13 g (50%). Anal. Calcd for C$_7$H$_{18}$Cl$_2$O$_4$RuS$_3$ (M_r = 434.37): C, 19.35; H, 4.17; S, 22.14. Found: C, 19.3; H, 4.13; S, 22.1. UV/visible spectra (λ_{max}, nm (ϵ, M^{-1} cm^{-1})): in CHCl$_3$ solution, 438 (sh, 90), 376 (251). Selected IR absorption bands: Nujol, ν_{CO} 1979 cm^{-1} (vs), ν_{SO} 1116 (vs) (DM*S*O), ν_{SO} 947 (s) (DMS*O*), ν_{Ru-O} 459 cm^{-1} (m), ν_{Ru-S} 414

Table 5. Positional Parameters and *B* Values with Estimated Standard Deviations for **5**

atom	*x*	*y*	*z*	B_{eq},[a] Å^2
RuA	0.9142(1)	0.500	0.9779(1)	1.99(1)
Cl1A	1.0679(4)	0.4608(1)	0.8001(4)	3.20(6)
Cl2A	0.7669(4)	0.5431(2)	1.1555(4)	4.25(7)
S1A	1.1509(4)	0.4770(1)	1.2174(4)	3.13(6)
S2A	0.6790(4)	0.5343(1)	0.7521(4)	2.72(6)
S3A	1.1177(4)	0.6063(1)	1.0905(4)	3.04(6)
O1A	1.262(1)	0.5200(4)	1.307(1)	5.0(2)
O2A	0.658(1)	0.5899(4)	0.749(1)	4.1(2)
O3A	1.0814(9)	0.5638(3)	0.9614(8)	2.5(2)
O4A	0.688(1)	0.4089(4)	0.981(1)	5.5(3)
C1A	1.054(3)	0.4462(7)	1.358(2)	6.4(5)
C2A	1.312(2)	0.4336(8)	1.185(2)	7.7(5)
C3A	0.701(2)	0.5162(7)	0.554(2)	5.2(4)
C4A	0.459(2)	0.5073(7)	0.737(2)	5.3(3)
C5A	1.354(2)	0.6232(5)	1.107(2)	5.3(4)
C6A	0.999(2)	0.6590(5)	0.978(2)	4.0(3)
C7A	0.776(1)	0.4448(5)	0.977(1)	2.8(2)
RuB	0.8149(1)	0.28345(4)	0.4927(1)	2.08(1)
Cl1B	0.6489(4)	0.2441(1)	0.6626(4)	3.52(6)
Cl2B	0.9933(4)	0.3136(1)	0.3197(4)	3.81(7)
S1B	0.5554(4)	0.2767(1)	0.2518(3)	2.76(6)
S2B	1.0749(3)	0.2913(1)	0.7322(3)	2.59(5)
S3B	0.9554(4)	0.1682(1)	0.5612(4)	2.82(6)
O1B	0.455(1)	0.3225(4)	0.189(1)	5.0(2)
O2B	1.168(1)	0.2434(4)	0.802(1)	4.4(2)
O3B	0.900(1)	0.2106(3)	0.4347(9)	2.9(2)
O4B	0.666(1)	0.3831(4)	0.545(1)	5.3(3)
C1B	0.619(2)	0.2506(8)	0.088(2)	7.1(5)
C2B	0.383(2)	0.2341(6)	0.265(2)	4.7(4)
C3B	1.011(2)	0.3206(6)	0.895(1)	3.7(3)
C4B	1.251(2)	0.3323(5)	0.709(2)	3.7(3)
C5B	1.190(2)	0.1525(6)	0.561(2)	4.3(3)
C6B	0.834(2)	0.1147(5)	0.450(2)	4.4(3)
C7B	0.726(2)	0.3451(5)	0.526(2)	3.7(3)

[a] Values for anisotropically refined atoms are given in the from of the isotropic equivalent displacement parameter defined as $(4/3)[a^2\beta(1,1) + b^2\beta(2,2) + c^2\beta(3,3) + ab(\cos\gamma)\beta(1,2) + ac(\cos\beta)\beta(1,3) + bc(\cos\alpha)\beta(2,3)]$.

Table 6. Positional Parameters and *B* Values with Estimated Standard Deviations for **7**

atom	*x*	*y*	*z*	B_{eq},[a] Å^2
Ru	0.23187(2)	0.27031(2)	0.25726(1)	1.976(3)
Cl2	0.07638(9)	0.38681(8)	0.39386(4)	3.42(1)
Cl1	−0.04881(8)	0.15553(7)	0.22781(5)	3.28(1)
S1	0.10400(8)	0.53404(7)	0.17762(4)	2.66(1)
S2	0.37222(8)	0.14750(7)	0.12693(4)	2.379(9)
O1	0.5587(3)	0.4156(3)	0.3138(2)	4.46(4)
O11	0.1524(3)	0.5615(2)	0.0788(1)	3.98(4)
O21	0.4775(3)	−0.0344(2)	0.1399(1)	3.34(3)
N1	0.3430(3)	0.0370(2)	0.3419(1)	2.56(3)
C1	0.4412(3)	0.3583(3)	0.2886(2)	2.76(4)
C2	0.2264(4)	−0.0359(3)	0.3996(2)	3.22(5)
C3	0.2947(5)	−0.1807(3)	0.4605(2)	4.19(6)
C4	0.4875(5)	−0.2504(4)	0.4621(2)	4.58(7)
C5	0.6078(4)	−0.1767(4)	0.4040(2)	4.14(6)
C6	0.5321(4)	−0.0337(3)	0.3445(2)	3.20(5)
C11	0.1667(5)	0.7045(3)	0.2321(2)	5.07(7)
C12	−0.1492(4)	0.5872(4)	0.1897(2)	4.74(7)
C21	0.2050(4)	0.1582(4)	0.0372(2)	3.92(6)
C22	0.5329(4)	0.2684(3)	0.0701(2)	3.57(5)

[a] Values for anisotropically refined atoms are given in the from of the isotropic equivalent displacement parameter defined as $(4/3)[a^2\beta(1,1) + b^2\beta(2,2) + c^2\beta(3,3) + ab(\cos\gamma)\beta(1,2) + ac(\cos\beta)\beta(1,3) + bc(\cos\alpha)\beta(2,3)]$.

Table 7. Positional Parameters and *B* Values with Estimated Standard Deviations for **9**

atom	*x*	*y*	*z*	B_{eq},[a] Å^2
RuA	0.34154(3)	0.17639(2)	0.26642(1)	2.068(4)
Cl1A	0.2489(1)	0.00467(6)	0.13647(6)	3.34(1)
Cl2A	0.0681(1)	0.15721(7)	0.32797(6)	3.58(2)
S1A	0.43690(9)	0.08279(6)	0.37386(5)	2.60(1)
N1A	0.2361(3)	0.2573(2)	0.1686(2)	2.50(4)
C1A	0.4099(4)	0.3104(3)	0.3682(2)	3.06(6)
C2A	0.5509(4)	0.1903(3)	0.2168(2)	3.35(6)
O1A	0.4515(4)	0.3916(2)	0.4288(2)	5.04(7)
O2A	0.6773(4)	0.1984(3)	0.1850(2)	6.15(7)
O11A	0.4878(4)	0.1483(2)	0.4787(2)	4.17(6)
C11A	0.2829(6)	−0.0340(3)	0.3688(3)	4.30(8)
C12A	0.6110(5)	0.0197(3)	0.3341(3)	4.98(8)
C3A	0.0766(4)	0.2181(3)	0.1213(2)	3.09(6)
C4A	0.0021(4)	0.2660(3)	0.0551(3)	3.83(7)
C5A	0.0950(5)	0.3572(3)	0.0381(2)	3.94(7)
C6A	0.2577(5)	0.3978(3)	0.0864(2)	3.78(7)
C7A	0.3272(4)	0.3461(3)	0.1517(2)	3.13(6)
RuB	0.17267(3)	0.33284(2)	0.72266(1)	2.138(4)
Cl1B	0.2622(1)	0.50301(7)	0.85497(6)	3.46(2)
Cl2B	−0.10318(9)	0.30716(6)	0.78060(5)	2.97(1)
S1B	0.05640(9)	0.42466(6)	0.62061(5)	2.65(1)
N1B	0.2751(3)	0.2496(2)	0.8208(2)	2.69(4)
C1B	0.1146(4)	0.1988(2)	0.6232(2)	2.73(5)
C2B	0.3862(4)	0.3641(3)	0.6788(2)	3.14(6)
O1B	0.0840(4)	0.1158(2)	0.5639(2)	4.38(6)
O2B	0.5163(3)	0.3856(3)	0.6542(2)	4.83(6)
O11B	0.1783(3)	0.4699(2)	0.5635(2)	4.48(5)
C11B	−0.0435(5)	0.5314(3)	0.6852(3)	3.94(7)
C12B	−0.1217(5)	0.3374(3)	0.5368(3)	3.81(7)
C3B	0.4371(4)	0.2816(3)	0.8648(3)	3.85(7)
C4B	0.5073(5)	0.2285(4)	0.9278(3)	4.96(8)
C5B	0.4071(5)	0.1406(3)	0.9454(3)	4.36(7)
C6B	0.2412(5)	0.1080(3)	0.9006(2)	3.82(7)
C7B	0.1780(4)	0.1638(3)	0.8379(2)	3.15(6)

[a] Values for anisotropically refined atoms are given in the from of the isotropic equivalent displacement parameter defined as $(4/3)[a^2\beta(1,1) + b^2\beta(2,2) + c^2\beta(3,3) + ab(\cos\gamma)\beta(1,2) + ac(\cos\beta)\beta(1,3) + bc(\cos\alpha)\beta(2,3)]$.

cm^{-1} (m), ν_{Ru-Cl} 340 cm^{-1} (vs); $CHCl_3$ solution, ν_{CO} 1983 cm^{-1} (vs). ^1H NMR spectrum in $CDCl_3$: 3.33 (s, 12, DM*S*O), 2.82 ppm (s, 6, DMS*O*). ^{13}C NMR spectrum in $CDCl_3$: 197.0 (1, CO), 44.1 (4, DM*S*O), 38.4 (2, DMS*O*).

***cis,cis,trans*-Ru(CO)$_2$(DMS*O*)$_2$Cl$_2$ (6).** A 0.3 g amount of *trans*-$RuCl_2$(DM*S*O)$_4$ (0.62 mmol) was partially dissolved in 18 mL of methanol and reacted with CO for 24 h. The clear, yellow solution obtained was concentrated to 2 mL and stored at 4 °C after addition of some diethyl ether. Yellow crystals of the product formed in a few hours and were then filtered, rapidly washed with cold methanol and diethyl ether, and vacuum dried. Yield: 0.12 g (50%). Anal. Calcd for $C_6H_{12}Cl_2O_4RuS_2$ (M_r = 384.25): C, 18.75; H, 3.14; S, 16.68. Found: C, 18.5; H, 3.06; S, 16.5. UV/visible spectra (λ_{max}, nm (ϵ, M^{-1} cm^{-1})): in $CHCl_3$ solution, 370 (669), 310 (292). Selected IR absorption bands: Nujol, ν_{CO} 2054, 1984 cm^{-1} (vs), ν_{SO} 951 (s) (DMS*O*), ν_{Ru-O} 470, 460 cm^{-1} (m), ν_{Ru-Cl} 331 cm^{-1} (vs); $CHCl_3$ solution, ν_{CO} 2067, 1998 cm^{-1} (vs). ^1H NMR spectrum in $CDCl_3$: 2.90 ppm (s, 12, DMS*O*). ^{13}C NMR spectrum in $CDCl_3$: 194.0 (2, CO), 39.2 (4, DMS*O*).

***cis,cis,cis*-Ru(CO)(py)(DM*S*O)$_2$Cl$_2$ (7).** A 0.22 g amount of **1** (0.5 mmol) was partially dissolved in 7 mL of methanol and 60 μL of py (0.75 mmol) was added. The mixture was heated to reflux for 5 min and a clear pale-yellow solution was obtained. The product precipitated as a pale yellow solid upon cooling to room temperature. It was then filtered, washed with cold methanol and diethyl ether, and vacuum dried. Yield: 0.11 g (50%). Anal. Calcd for $C_{10}H_{17}Cl_2NO_3RuS_2$ (M_r = 435.34): C, 27.58; H, 3.93; N, 3.21. Found: C, 27.3; H, 3.84; N, 3.27. Selected IR absorption bands: Nujol, ν_{CO} 2001 cm^{-1} (vs), ν_{SO} 1110, 1098 (s) (DM*S*O), ν_{Ru-S} 425 cm^{-1} (m), ν_{Ru-Cl} 330, 286 cm^{-1} (m). ^1H NMR spectrum in $CDCl_3$ (methyl peaks were assigned to either $DMSO_a$ or $DMSO_b$ according to a NOESY spectrum): 9.07 (m, 2, Hα), 7.82 (m, 1, Hγ), 7.38 (m, 2, Hβ), 3.55 (s, 3, DM*S*O$_a$), 3.52 (s, 3, DM*S*O$_a$), 3.51 (s, 3, DM*S*O$_b$), 3.33 ppm (s, 3, DM*S*O$_b$). ^{13}C NMR spectrum in $CDCl_3$: 194.0 (1, CO), 155.8 (2, py), 138.4 (1, py), 124.6 (2, py), 49.0 (1, DM*S*O), 48.9 (1, DM*S*O), 44.9 (1, DM*S*O), 44.6 ppm (1, DM*S*O).

Table 8. Selected Bond Distances (Å) and Angles (deg) for **1**

Bond Distances			
Molecule **A**			
Ru1−Cl1A	2.398(2)	S1A−C2A	1.770(8)
Ru1−Cl2A	2.418(2)	S2A−O2A	1.459(6)
Ru1−S1A	2.280(2)	S2A−C3A	1.760(9)
Ru1−S2A	2.297(2)	S2A−C4A	1.775(7)
Ru1−O3A	2.139(5)	S3A−O3A	1.545(4)
Ru1−C7A	1.838(7)	S3A−C5A	1.76(1)
S1A−O1A	1.469(5)	S3A−C6A	1.77(1)
S1A−C1A	1.767(9)	O4A−C7A	1.132(9)
Molecule **B**			
Ru2−Cl1B	2.405(2)	S1B−C2B	1.776(9)
Ru2−Cl2B	2.413(2)	S2B−O2B	1.463(6)
Ru2−S1B	2.279(2)	S2B−C3B	1.777(7)
Ru2−S2B	2.303(2)	S2B−C4B	1.754(9)
Ru2−O3B	2.134(5)	S3B−O3B	1.544(5)
Ru2−C7B	1.838(7)	S3B−C5B	1.75(1)
S1B−O1B	1.460(5)	S3B−C6B	1.75(1)
S1B−C1B	1.775(9)	O4B−C7B	1.137(9)
Bond Angles			
Molecule **A**			
Cl1A−Ru1−Cl2A	87.52(6)	Ru1−S1A−C1A	110.9(3)
Cl1A−Ru1−S1A	88.73(6)	Ru1−S1A−C2A	113.2(2)
Cl1A−Ru1−S2A	175.93(7)	O1A−S1A−C1A	108.5(3)
Cl1A−Ru1−O3A	89.8(1)	O1A−S1A−C2A	106.5(3)
Cl1A−Ru1−C7A	92.9(2)	C1A−S1A−C2A	99.8(4)
Cl2A−Ru1−S1A	176.25(6)	Ru1−S2A−O2A	117.4(2)
Cl2A−Ru1−S2A	91.87(6)	Ru1−S2A−C3A	111.7(3)
Cl2A−Ru1−O3A	89.1(1)	Ru1−S2A−C4A	112.5(3)
Cl2A−Ru1−C7A	87.8(2)	O2A−S2A−C3A	107.1(4)
S1A−Ru1−S2A	91.86(6)	O2A−S2A−C4A	108.4(3)
S1A−Ru1−O3A	90.8(1)	C3A−S2A−C4A	98.0(4)
S1A−Ru1−C7A	92.5(2)	O3A−S3A−C5A	104.5(3)
S2A−Ru1−O3A	86.2(1)	O3A−S3A−C6A	102.0(3)
S2A−Ru1−C7A	91.1(2)	C5A−S3A−C6A	98.7(5)
O3A−Ru1−C7A	175.8(3)	Ru1−O3A−S3A	122.3(2)
Ru1−S1A−O1A	116.6(2)	Ru1−C7A−O4A	176.4(6)
Molecule **B**			
Cl1B−Ru2−Cl2B	88.50(7)	Ru2−S1B−C1B	112.2(2)
Cl1B−Ru2−S1B	88.42(6)	Ru2−S1B−C2B	110.5(3)
Cl1B−Ru2−S2B	176.47(8)	O1B−S1B−C1B	107.1(3)
Cl1B−Ru2−O3B	89.1(1)	O1B−S1B−C2B	107.9(3)
Cl1B−Ru2−C7B	92.1(2)	C1B−S1B−C2B	100.4(4)
Cl2B−Ru2−S1B	176.91(7)	Ru2−S2B−O2B	117.3(2)
Cl2B−Ru2−S2B	90.97(6)	Ru2−S2B−C3B	111.8(3)
Cl2B−Ru2−O3B	88.9(1)	Ru2−S2B−C4B	112.4(3)
Cl2B−Ru2−C7B	87.9(2)	O2B−S2B−C3B	108.5(3)
S1B−Ru2−S2B	92.12(6)	O2B−S2B−C4B	107.0(4)
S1B−Ru2−O3B	91.3(1)	C3B−S2B−C4B	98.0(4)
S1B−Ru2−C7B	92.0(2)	O3B−S3B−C5B	103.9(3)
S2B−Ru2−O3B	87.4(1)	O3B−S3B−C6B	104.2(4)
S2B−Ru2−C7B	91.3(2)	C5B−S3B−C6B	98.7(6)
O3B−Ru2−C7B	176.6(2)	Ru2−O3B−S3B	120.7(2)
Ru2−S1B−O1B	117.4(2)	Ru2−C7B−O4B	176.0(5)

Table 9. Selected Bond Distances (Å) and Angles (deg) for **3**

Bond Distances			
RuA−Cl1A	2.392(1)	RuB−Cl1B	2.393(1)
RuA−Cl2A	2.403(1)	RuB−Cl2B	2.408(1)
RuA−S1A	2.364(1)	RuB−S1B	2.358(1)
RuA−S2A	2.354(1)	RuB−S2B	2.355(1)
RuA−C1A	1.884(5)	RuB−C1B	1.888(5)
RuA−C2A	1.888(6)	RuB−C2B	1.885(5)
S1A−C11A	1.467(4)	S1B−O11B	1.463(4)
S1A−C12A	1.772(7)	S1B−C11B	1.766(5)
S1A−C11A	1.779(6)	S1B−C12B	1.769(6)
S2A−O21A	1.460(4)	S2B−O21B	1.476(4)
S2A−C21A	1.771(7)	S2B−C21B	1.785(6)
S2A−C22A	1.766(7)	S2B−C22B	1.776(6)
O1A−C1A	1.138(7)	O1B−C1B	1.128(7)
O2A−C2A	1.120(8)	O2B−C2B	1.121(7)
Bond Angles			
Cl1A−RuA−Cl2A	91.07(5)	Cl1B−RuB−Cl2B	91.71(5)
Cl1A−RuA−S1A	90.00(5)	Cl1B−RuB−S1B	87.06(4)
Cl1A−RuA−S2A	91.22(5)	Cl1B−RuB−S2B	88.97(5)
Cl1A−RuA−C1A	85.9(2)	Cl1B−RuB−C1B	176.5(2)
Cl1A−RuA−C2A	178.7(2)	Cl1B−RuB−C2B	87.7(2)
Cl2A−RuA−S1A	90.47(4)	Cl2B−RuB−S1B	90.34(5)
Cl2A−RuA−S2A	84.63(5)	Cl2B−RuB−S2B	90.49(5)
Cl2A−RuA−C1A	176.8(2)	Cl2B−RuB−C1B	85.1(2)
Cl2A−RuA−C2A	89.7(2)	Cl2B−RuB−C2B	177.9(2)
S1A−RuA−S2A	174.97(4)	S1B−RuB−S2B	175.97(4)
S1A−RuA−C1A	90.6(2)	S1B−RuB−C1B	94.6(2)
S1A−RuA−C2A	89.0(2)	S1B−RuB−C2B	87.6(2)
S2A−RuA−C1A	94.3(2)	S2B−RuB−C1B	89.4(2)
S2A−RuA−C2A	89.8(2)	S2B−RuB−C2B	91.5(2)
C1A−RuA−C2A	93.3(2)	C1B−RuB−C2B	95.5(2)
RuA−S1A−O11A	114.9(2)	RuB−S1B−O11B	113.6(2)
RuA−S1A−C12A	112.5(2)	RuB−S1B−C11B	111.4(3)
RuA−S1A−C11A	110.5(2)	RuB−S1B−C12B	112.3(2)
O11A−S1A−C12A	108.3(3)	O11B−S1B−C11B	109.1(3)
O11A−S1A−C11A	109.4(3)	O11B−S1B−C12B	108.5(3)
C12A−S1A−C11A	100.3(3)	C11B−S1B−C12B	101.3(3)
RuA−S2A−O21A	115.0(2)	RuB−S2B−O21B	115.1(2)
RuA−S2A−C21A	112.4(2)	RuB−S2B−C21B	111.9(2)
RuA−S2A−C22A	110.3(2)	RuB−S2B−C22B	111.5(2)
O21A−S2A−C21A	108.4(3)	O21B−S2B−C21B	108.9(3)
O21A−S2A−C22A	108.5(3)	O21B−S2B−C22B	108.8(3)
C21A−S2A−C22A	101.3(3)	C21B−S2B−C22B	99.5(3)
RuA−C1A−O1A	178.6(5)	RuB−C1B−O1B	175.3(5)
RuA−C2A−O2A	179.2(5)	RuB−C2B−O2B	177.1(5)

Table 10. Selected Bond Distances (Å) and Angles (deg) for **4**

Bond Distances			
Ru−Cl1	2.382(1)	S−O4	1.535(4)
Ru−Cl2	2.404(1)	S−C4	1.763(6)
Ru−O4	2.095(4)	S−C5	1.773(6)
Ru−C1	1.892(6)	O1−C1	1.125(7)
Ru−C2	1.911(5)	O2−C2	1.113(7)
Ru−C3	1.879(6)	O3−C3	1.137(8)
Bond Angles			
Cl1−Ru−Cl2	90.40(5)	O4−Ru−C3	178.2(2)
Cl1−Ru−O4	89.8(1)	C1−Ru−C2	93.0(2)
Cl1−Ru−C1	177.2(2)	C1−Ru−C3	92.3(2)
Cl1−Ru−C2	88.1(2)	C2−Ru−C3	92.6(2)
Cl1−Ru−C3	90.2(2)	O4−S−C4	103.0(3)
Cl2−Ru−O4	88.3(1)	O4−S−C5	103.3(3)
Cl2−Ru−C1	88.4(2)	C4−S−C5	100.1(3)
Cl2−Ru−C2	177.2(2)	Ru−O4−S	120.0(2)
Cl2−Ru−C3	89.8(2)	Ru−C1−O1	178.0(5)
O4−Ru−C1	87.7(2)	Ru−C2−O2	178.6(5)
O4−Ru−C2	89.3(2)	Ru−C3−O3	175.9(5)

***cis,cis,cis*-Ru(CO)$_2$(py)(DMSO)Cl$_2$ (8).** A 0.19 g amount of **3** (0.5 mmol) was partially dissolved in 10 mL of methanol, and 80 μL of py (1 mmol) was added. The mixture was stirred for 1 h at room temperature, until a clear colorless solution was obtained. Its volume was reduced under vacuum to approximately two-thirds, when the product precipitated as white microcrystals. It was then filtered, washed with cold methanol and diethyl ether, and vacuum dried. Yield: 0.14 g (73%). Anal. Calcd for $C_9H_{11}Cl_2NO_3RuS$ ($M_r = 385.22$): C, 28.06; H, 2.87; N, 3.63. Found: C, 27.9; H, 2.85; N, 3.66. Selected IR absorption bands: Nujol, ν_{CO} 2089, 2036 cm^{-1} (vs), ν_{SO} 1126 (s) (DMSO), ν_{Ru-S} 421 cm^{-1} (m), ν_{Ru-Cl} 324, 300 cm^{-1} (m). ^{1}H NMR spectrum in CDCl$_3$: 9.21 (m, 2, Hα), 8.02 (m, 1, Hγ), 7.59 (m, 2, Hβ), 3.50 (s, 3, DMSO), 2.87 (s, 3, DMSO). ^{13}C NMR spectrum in CDCl$_3$: 191.4 (1, CO), 187.4 (1, CO), 153.8 (2, py), 139.6 (1, py), 125.9 (2, py), 50.2 (1, DMSO), 43.9 (1, DMSO).

***cis,trans,cis*-Ru(CO)$_2$(py)(DMSO)Cl$_2$ (9).** The above reaction was repeated in a 2-fold amount of methanol and concentration was avoided. A small amount of **8** precipitated in a few hours and was removed by filtration. The mother liquor was then concentrated in vacuum to 5 mL and some diethyl ether was added. Colorless crystals of **9** were obtained overnight and were then filtered, washed with cold methanol and diethyl ether, and vacuum dried. Yield: 0.10 g (55%). Anal. Calcd for $C_9H_{11}Cl_2NO_3RuS$ (M_r = 385.22): C, 28.06; H, 2.87; N, 3.63. Found: C, 27.8; H, 2.78; N, 3.56. Selected IR absorption bands: Nujol, ν_{CO} 2076, 2010 cm^{-1} (vs), ν_{SO} 1134 (s) (DMSO), ν_{Ru-S} 422 cm^{-1} (m),

Table 11. Selected Bond Distances (Å) and Angles (deg) for **5**

	Bond Distances		
RuA−Cl1A	2.375(3)	RuB−Cl1B	2.388(4)
RuA−Cl2A	2.391(4)	RuB−Cl2B	2.379(4)
RuA−S1A	2.315(3)	RuB−S1B	2.337(2)
RuA−S2A	2.340(3)	RuB−S2B	2.334(2)
RuA−O3A	2.142(8)	RuB−O3B	2.151(8)
RuA−C7A	1.80(1)	RuB−C7B	1.83(1)
S1A−O1A	1.48(1)	S1B−O1B	1.45(1)
S1A−C1A	1.76(2)	S1B−C1B	1.73(2)
S1A−C2A	1.75(2)	S1B−C2B	1.75(2)
S2A−O2A	1.50(1)	S2B−O2B	1.49(1)
S2A−C3A	1.78(2)	S2B−C3B	1.76(1)
S2A−C4A	1.75(1)	S2B−C4B	1.76(1)
S3A−O3A	1.536(8)	S3B−O3B	1.524(8)
S3A−C5A	1.77(1)	S3B−C5B	1.79(1)
S3A−C6A	1.78(1)	S3B−C6B	1.80(1)
O4A−C7A	1.16(2)	O4B−C7B	1.14(2)
	Bond Angles		
Cl1A−RuA−Cl2A	177.3(1)	Cl1B−RuB−Cl2B	173.6(1)
Cl1A−RuA−S1A	92.4(1)	Cl1B−RuB−S1B	92.3(1)
Cl1A−RuA−S2A	92.9(1)	Cl1B−RuB−S2B	88.3(1)
Cl1A−RuA−O3A	85.2(2)	Cl1B−RuB−O3B	88.4(2)
Cl1A−RuA−C7A	90.9(4)	Cl1B−RuB−C7B	92.0(5)
Cl2A−RuA−S1A	87.7(1)	Cl2B−RuB−S1B	88.1(1)
Cl2A−RuA−S2A	86.7(1)	Cl2B−RuB−S2B	91.4(1)
Cl2A−RuA−O3A	92.1(2)	Cl2B−RuB−O3B	85.2(2)
Cl2A−RuA−C7A	91.8(4)	Cl2B−RuB−C7B	94.4(5)
S1A−RuA−S2A	172.1(1)	S1B−RuB−S2B	179.2(1)
S1A−RuA−O3A	88.1(2)	S1B−RuB−O3B	87.5(2)
S1A−RuA−C7A	93.8(3)	S1B−RuB−C7B	87.6(3)
S2A−RuA−O3A	86.5(2)	S2B−RuB−O3B	93.1(2)
S2A−RuA−C7A	92.0(3)	S2B−RuB−C7B	91.8(3)
O3A−RuA−C7A	175.8(4)	O3B−RuB−C7B	175.1(4)
RuA−S1A−O1A	112.9(4)	RuB−S1B−O1B	116.6(4)
RuA−S1A−C1A	110.4(6)	RuB−S1B−C1B	111.4(4)
RuA−S1A−C2A	114.7(6)	RuB−S1B−C2B	115.3(5)
O1A−S1A−C1A	107.7(7)	O1B−S1B−C1B	106.7(8)
O1A−S1A−C2A	107.1(7)	O1B−S1B−C2B	105.6(6)
C1A−S1A−C2A	103(1)	C1B−S1B−C2B	99.6(8)
RuA−S2A−O2A	117.0(3)	RuB−S2B−O2B	115.0(4)
RuA−S2A−C3A	113.0(5)	RuB−S2B−C3B	111.1(4)
RuA−S2A−C4A	110.3(5)	RuB−S2B−C4B	114.3(4)
O2A−S2A−C3A	106.9(7)	O2B−S2B−C3B	106.5(6)
O2A−S2A−C4A	108.8(7)	O2B−S2B−C4B	107.9(6)
C3A−S2A−C4A	99.3(7)	C3B−S2B−C4B	100.9(7)
O3A−S3A−C5A	101.8(6)	O3B−S3B−C5B	103.6(6)
O3A−S3A−C6A	105.3(5)	O3B−S3B−C6B	104.4(5)
C5A−S3A−C6A	99.2(7)	C5B−S3B−C6B	98.6(7)
RuA−O3A−S3A	121.9(5)	RuB−O3B−S3B	123.9(5)
RuA−C7A−O4A	178.4(9)	RuB−C7B−O4B	179(1)

$\nu_{\text{Ru-Cl}}$ 311, 291 cm^{-1} (m). ^{1}H NMR spectrum in $CDCl_3$: 8.90 (m, 2, Hα), 7.90 (m, 1, Hγ), 7.45 (m, 2, Hβ), 3.52 (s, 6, DM*S*O). ^{13}C NMR spectrum in $CDCl_3$: 188.4 (2, CO), 155.1 (2, py), 139.1 (1, py), 125.9 (2, py), 46.8 (2, DM*S*O).

***cis,cis,trans*-Ru(CO)$_2$(py)$_2$Cl$_2$ (10).** A 0.19 g amount of **3** (0.5 mmol) was partially dissolved in 20 mL of methanol, and 0.24 mL of py (6 mmol) was added. The mixture was heated to reflux for 6 h. Upon heating, the clear colorless solution obtained in few minutes turned gradually pale yellow. Crystal of **10** were obtained in two days from the solution stored at room temperature. They were filtered, washed with cold acetone and diethyl ether, and vacuum dried. Yield: 0.12 g (60%). Anal. Calcd for $C_{12}H_{10}Cl_2N_2O_2Ru$ (M_r = 386.19): C, 37.32; H, 2.61; N, 7.25. Found: C, 37.1; H, 2.54; N, 7.22. Selected IR absorption bands: Nujol, ν_{CO} 2055, 1987 cm^{-1} (vs), $\nu_{\text{Ru-Cl}}$ 332 cm^{-1} (s). ^{1}H NMR spectrum in $CDCl_3$: 8.88 (m, 4, Hα), 7.88 (m, 2, Hγ), 7.41 (m, 4, Hβ). ^{13}C NMR spectrum in $CDCl_3$: 194.8 (2, CO), 152.6 (4, py), 138.7 (2, py), 125.1 (4, py).

Complex **10** was obtained also upon reaction of **6** with pyridine. A 0.20 g amount of **6** (0.5 mmol) was dissolved in 5 mL of methanol and reacted at room temperature with 0.16 mL of py (2 mmol). Yellow microcrystals of the product precipitated from the solution within 1 h. They were filtered, washed with cold methanol and diethyl ether, and vacuum dried. Yield: 0.1 g (50%).

Table 12. Selected Bond Distances (Å) and Angles (deg) for **7**

	Bond Distances		
Ru−Cl2	2.4035(6)	S2−C21	1.778(3)
Ru−Cl1	2.4296(7)	S2−C22	1.778(3)
Ru−S1	2.3128(5)	O1−C1	1.119(3)
Ru−S2	2.3095(5)	N1−C2	1.339(3)
Ru−N1	2.140(2)	N1−C6	1.347(3)
Ru−C1	1.859(3)	C2−C3	1.392(3)
S1−O11	1.471(2)	C3−C4	1.369(5)
S1−C11	1.767(3)	C4−C5	1.364(5)
S1−C12	1.771(3)	C5−C6	1.382(3)
S2−O21	1.476(2)		
	Bond Angles		
Cl2−Ru−Cl1	89.64(2)	O11−S1−C11	106.6(1)
Cl2−Ru−S1	87.44(2)	O11−S1−C12	107.9(1)
Cl2−Ru−S2	177.08(2)	C11−S1−C12	100.4(2)
Cl2−Ru−N1	87.65(5)	Ru−S2−O21	116.74(7)
Cl2−Ru−C1	86.59(7)	Ru−S2−C21	112.70(9)
Cl1−Ru−S1	91.86(2)	Ru−S2−C22	112.21(9)
Cl1−Ru−S2	87.78(2)	O21−S2−C21	106.6(1)
Cl1−Ru−N1	89.19(6)	O21−S2−C22	106.8(1)
Cl1−Ru−C1	175.92(7)	C21−S2−C22	100.3(1)
S1−Ru−S2	94.00(2)	Ru−N1−C2	120.3(1)
S1−Ru−N1	174.97(5)	Ru−N1−C6	121.8(2)
S1−Ru−C1	89.53(7)	C2−N1−C6	117.8(2)
S2−Ru−N1	90.95(5)	Ru−C1−O1	174.3(2)
S2−Ru−C1	95.95(7)	N1−C2−C3	122.1(2)
N1−Ru−C1	89.10(9)	C2−C3−C4	119.1(3)
Ru−S1−O11	118.75(7)	C3−C4−C5	119.2(2)
Ru−S1−C11	110.1(1)	C4−C5−C6	119.2(3)
Ru−S1−C12	111.5(1)	N1−C6−C5	122.5(2)

***fac*-Ru(CO)$_3$(py)Cl$_2$ (11).** A 0.20 g amount of **4** (0.6 mmol) was dissolved in 5 mL of acetone and reacted for 30 min at room temperature with 0.19 mL of py (2.4 mmol). The pale yellow solution was then concentrated to 2 mL and stored at 4 °C after addition of some diethyl ether. White microcrystals of the product formed overnight and were then filtered, washed with cold acetone and diethyl ether, and vacuum dried. Yield: 0.23 g (60%). Anal. Calcd for $C_8H_5Cl_2NO_3Ru$ (M_r = 335.10): C, 28.67; H, 1.50; N, 4.17. Found: C, 28.4; H, 1.43; N, 4.12. Selected IR absorption bands: Nujol, ν_{CO} 2137, 2055 (br) cm^{-1} (vs), $\nu_{\text{Ru-Cl}}$ 322, 300 cm^{-1} (m). ^{1}H NMR spectrum in $CDCl_3$: 8.96 (m, 2, Hα), 8.00 (m, 1, Hγ), 7.56 (m, 2, Hβ). ^{13}C NMR spectrum in $CDCl_3$: 185.3 (1, CO), 184.7 (2, CO), 153.9 (2, py), 139.9 (1, py), 126.2 (2, py).

***cis,cis,trans*-Ru(CO)(DMSO)(py)$_2$Cl$_2$ (12).** A 0.22 g amount of **5** (0.5 mmol) was dissolved in 5 mL of methanol and reacted for 2 h at room temperature with 0.12 mL of py (1.5 mmol). The deep yellow solution was then concentrated to 2 mL and stored at 4 °C after addition of some diethyl ether. Yellow microcrystals of the product formed overnight and were then filtered, washed with cold methanol and diethyl ether, and vacuum dried. Yield: 0.1 g (45%). Anal. Calcd for $C_{13}H_{16}Cl_2N_2O_2RuS$ (M_r = 436.31): C, 35.78; H, 3.69; N, 6.42. Found: C, 35.5; H, 3.60; N, 6.38. Selected IR absorption bands: Nujol, ν_{CO} 1969 cm^{-1} (vs), ν_{SO} 1096 (s) (DMSO), $\nu_{\text{Ru-S}}$ 423 cm^{-1} (m), $\nu_{\text{Ru-Cl}}$ 343 cm^{-1} (s). ^{1}H NMR spectrum in $CDCl_3$ (signals of py**A** and py**B** were distinguished by a COSY spectrum): 9.17 (m, 2, HαA), 8.68 (m, 2, HαB), 7.85 (m, 1, HγA), 7.76 (m, 1, HγB), 7.39 (m, 2, HβA), 7.27 (m, 2, HβB), 3.38 ppm (s, 6, DM*S*O). ^{13}C NMR spectrum in $CDCl_3$: 200.4 (1, CO), 154.3 (2, py), 152.9 (2, py), 138.2 (1, py), 137.7 (1, py), 124.6 (2, py), 124.2 (2, py), 47.2 (2, DM*S*O).

Crystallographic Study. Crystals of complexes **1**, **3**, **4**, **5**, **7**, and **9**, suitable for X-ray structure determination, grew from the corresponding reaction mixtures. A summary of the crystal data and data collection and refinement is given in Table 1.

Intensities and cell parameters were determined with an Enraf-Nonius CAD-4 diffractometer, with the exception of **5**, for which a KUMA KM-4 diffractometer was used. All data sets were corrected for Lorentz and polarization effects, and for absorption employing ψ scans on three reflections with χ near 90°. In the case of **5**, an empirical correction (DIFABS) was used. All the structures were solved by the heavy-atom method through Patterson and Fourier syntheses and refined by full-matrix least-squares method, with anisotropic temperature factors

Table 13. Selected Bond Distances (Å) and Angles (deg) for **9**

	Bond Distances		
RuA−Cl1A	2.4110(7)	RuB−Cl1B	2.4123(7)
RuA−Cl2A	2.4114(8)	RuB−Cl2B	2.4118(8)
RuA−S1A	2.3269(9)	RuB−S1B	2.3171(8)
RuA−N1A	2.134(3)	RuB−N1B	2.149(3)
RuA−C1A	1.881(3)	RuB−C1B	1.861(2)
RuA−C2A	1.862(3)	RuB−C2B	1.878(3)
C1A−O1A	1.133(4)	C1B−O1B	1.137(3)
C2A−O2A	1.137(4)	C2B−O2B	1.136(4)
S1A−O11A	1.472(2)	S1B−O11B	1.465(3)
S1A−C11A	1.763(4)	S1B−C11B	1.769(4)
S1A−C12A	1.767(4)	S1B−C12B	1.771(3)
N1A−C3A	1.329(4)	N1B−C3B	1.327(4)
N1A−C7A	1.344(4)	N1B−C7B	1.337(4)
C3A−C4A	1.393(5)	C3B−C4B	1.390(6)
C4A−C5A	1.374(5)	C4B−C5B	1.372(6)
C5A−C6A	1.358(5)	C5B−C6B	1.358(5)
C6A−C7A	1.400(5)	C6B−C7B	1.391(5)
	Bond Angles		
S1A−RuA−Cl1A	90.26(3)	S1B−RuB−Cl1B	90.79(3)
S1A−RuA−Cl2A	87.76(3)	S1B−RuB−Cl2B	87.97(3)
S1A−RuA−N1A	175.99(7)	S1B−RuB−N1B	178.14(7)
S1A−RuA−C1A	89.9(1)	S1B−RuB−C1B	92.0(1)
S1A−RuA−C2A	92.8(1)	S1B−RuB−C2B	89.0(1)
Cl1A−RuA−Cl2A	91.28(3)	Cl1B−RuB−Cl2B	89.72(3)
Cl1A−RuA−N1A	88.38(6)	Cl1B−RuB−N1B	88.22(6)
Cl1A−RuA−C1A	179.0(1)	Cl1B−RuB−C1B	176.7(1)
Cl1A−RuA−C2A	88.02(9)	Cl1B−RuB−C2B	87.17(9)
Cl2A−RuA−N1A	88.50(7)	Cl2B−RuB−N1B	90.45(7)
Cl2A−RuA−C1A	87.8(1)	Cl2B−RuB−C1B	92.1(1)
Cl2A−RuA−C2A	179.10(9)	Cl2B−RuB−C2B	175.6(1)
N1A−RuA−C1A	91.4(1)	N1B−RuB−C1B	89.1(1)
N1A−RuA−C2A	90.9(1)	N1B−RuB−C2B	92.5(1)
C1A−RuA−C2A	92.9(1)	C1B−RuB−C2B	91.1(1)
RuA−S1A−O11A	116.0(1)	RuB−S1B−O11B	114.6(1)
RuA−S1A−C11A	111.4(1)	RuB−S1B−C11B	113.0(1)
RuA−S1A−C12A	111.9(2)	RuB−S1B−C12B	110.7(1)
O11A−S1A−C11A	108.4(2)	O11B−S1B−C11B	108.4(2)
O11A−S1A−C12A	107.7(2)	O11B−S1B−C12B	108.6(2)
C11A−S1A−C12A	100.3(2)	C11B−S1B−C12B	100.6(2)
RuA−C1A−O1A	179.3(3)	RuB−C1B−O1B	177.6(3)
RuA−C2A−O2A	178.9(3)	RuB−C2B−O2B	178.2(3)
RuA−N1A−C3A	119.4(2)	RuB−N1B−C3B	120.7(2)
RuA−N1A−C7A	122.0(2)	RuB−N1B−C7B	120.8(2)
C3A−N1A−C7A	118.7(3)	C3B−N1B−C7B	118.5(3)
N1A−C3A−C4A	122.0(3)	N1B−C3B−C4B	121.9(3)
N1A−C7A−C6A	121.6(3)	N1B−C7B−C6B	122.1(3)
C3A−C4A−C5A	119.4(3)	C3B−C4B−C5B	119.5(3)
C4A−C5A−C6A	118.9(4)	C4B−C5B−C6B	118.7(4)
C5A−C6A−C7A	119.5(3)	C5B−C6B−C7B	119.4(3)

for all non-hydrogen atoms. The hydrogen atoms were included at calculated positions and held fixed during refinement with isotropic *B* factors = $1.3B_{eq}$ of the carbon atoms to which they are bonded. All calculations were performed by using the MolEN suite of programs, as described in the preceding paper.[9] The final coordinates of non-hydrogen atoms are listed in Tables 2−7 for **1**, **3**, **4**, **5**, **7**, and **9**, respectively, while bond lengths and angles are given in Tables 8−13. The labeling schemes are shown in Figures 1−6.

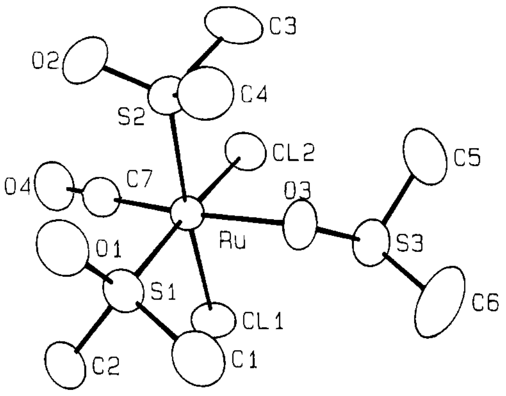

Figure 1. ORTEP drawing of **1** with the atom-labeling scheme.

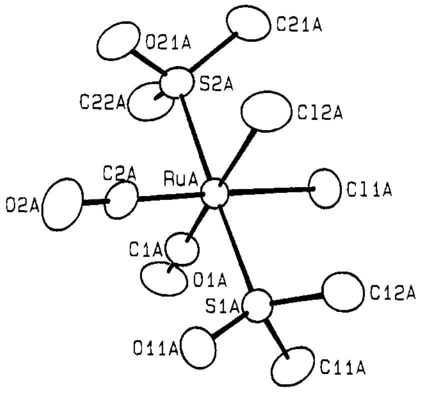

Figure 2. ORTEP drawing of **3** with the atom-labeling scheme.

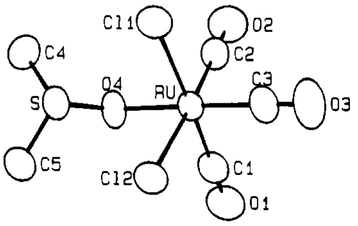

Figure 3. ORTEP drawing of **4** with the atom-labeling scheme.

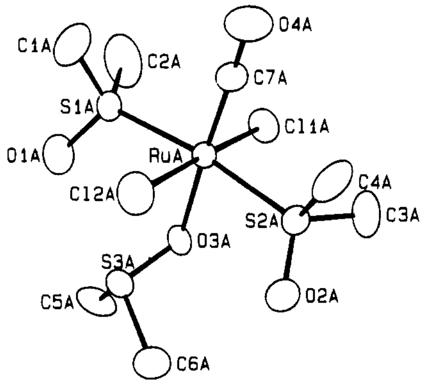

Figure 4. ORTEP drawing of **5** with the atom-labeling scheme.

Results

Reactions of *cis*-$RuCl_2(DMSO)_4$ with CO. The reaction between *cis*-$RuCl_2(DMSO)_4$ and CO at room temperature and ambient pressure was first monitored by ^1H NMR in $CDCl_3$. The signals of *cis*-$RuCl_2(DMSO)_4$ were slowly replaced by four equally intense peaks, two in the region of S-bonded DMSO, one in that of O-bonded DMSO (Table 14), and one corresponding to free DMSO. They were attributed to a monocarbonyl product (**1**). Complex **1** reached a maximum concentration in 3 h and was then slowly replaced by a transient disubstituted species (**2**) with an NMR spectrum characterized by four equally intense singlets, two in the region of S-bonded and two in that of O-bonded DMSO (Table 14). This spectral pattern, attributed to a *cis,cis,cis*-$Ru(CO)_2(DMSO)(DMSO)Cl_2$ species (see below), was gradually replaced by a single resonance for S-bonded DMSO (**3**) (Table 14). When the reaction was completed, in approximately 5 days, the new signal integrated as the signal of free DMSO, suggesting that also **3** must be disubstituted, with equivalent DMSO ligands. No further evolution of the spectrum was observed for longer observation times.

We have been able to isolate compounds **1**−**3** by a careful choice of the reaction conditions and solvent. The monocar-

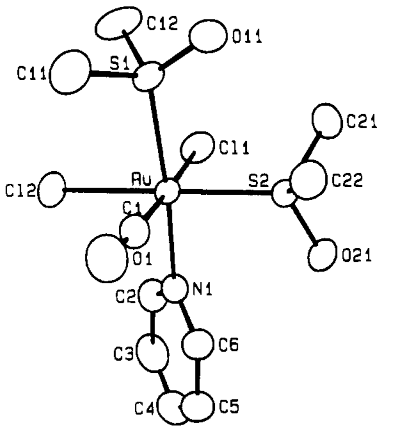

Figure 5. ORTEP drawing of **7** with the atom-labeling scheme.

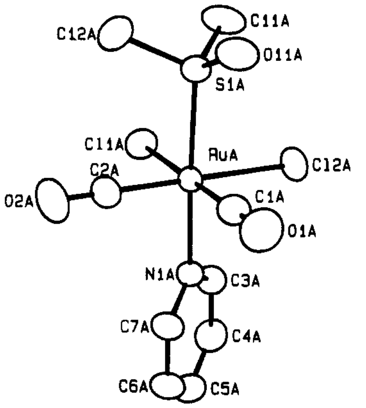

Figure 6. ORTEP drawing of **9** with the atom-labeling scheme.

bonyl species **1** was isolated in good yield from the concentrated solution when the reaction between *cis*-RuCl$_2$(DMSO)$_4$ and CO was run in methanol at room temperature and ambient pressure (eq 1). The presence of coordinated CO, beside that of both S-bonded and O-bonded DMSO ligands, was confirmed by the ^{13}C NMR and solid state IR spectra of **1** (Tables 15 and 16, respectively). (The solution IR spectral data for **1**−**6** were given in Table 17.) A cis disposition of the two chlorides was also suggested by the two Ru−Cl stretching bands. Comparison with the DMSO-d_6 derivative allowed a thorough assignment of the IR bands. The ^{1}H NMR pattern of **1** (see above), combined with IR evidence, was in agreement with a *trans,cis,cis*-Ru(CO)(DMS*O*)(DM*S*O)$_2$Cl$_2$ geometry for the complex, where the two chemically equivalent DM*S*O ligands have diastereotopic methyl groups. It also suggested that, as already observed in the Ru(III) derivatives,[9] coordination of CO induces the selective S to O linkage isomerization of the DM*S*O trans to it. The geometry of the complex was confirmed by the X-ray crystal structure reported in Figure 1.

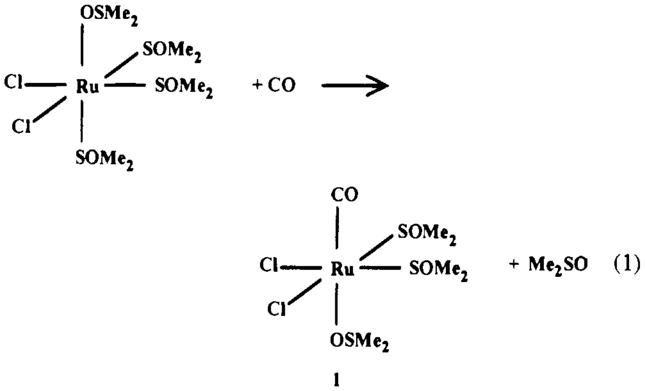

1

Table 14. ^{1}H Chemical Shifts of Compounds **1**−**6** in CDCl$_3$ Solution (ppm)

complex	DM*S*O	DMS*O*
1	3.43 (s, 6), 3.26 (s, 6)	2.85 (6)
2	3.42 (s, 3), 3.17 (s, 3)	2.89 (s, 3), 2.86 (s, 3)
3	3.44 (s, 12)	
4		2.86 (s, 6)
5	3.33 (s, 12)	2.82 (s, 6)
6		2.90 (s, 12)

Table 15. ^{13}C Chemical Shifts of Compounds **1**−**6** in CDCl$_3$ Solution (ppm)

complex	CO	DM*S*O	DMS*O*
1	196.3 (1)	47.6 (2), 46.7 (2)	39.1 (2)
2	191.9 (1), 186.1 (1)	47.4 (1), 42.3 (1)	39.2 (1), 38.9 (1)
3	185.6 (2)	45.1 (4)	
4	186.7 (1), 183.4 (2)		39.1 (2)
5	197.9 (1)	44.1 (4)	38.4 (2)
6	194.4 (2)		39.2 (4)

Longer reaction times allowed the isolation, in low yield, of the thermodynamically unstable disubstituted species **2** (eq 2).

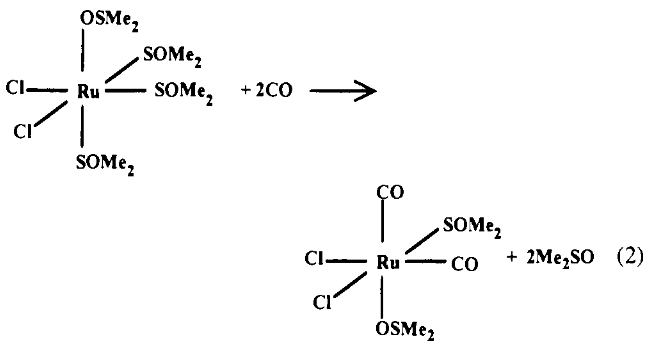

2

The solid state IR spectrum confirmed the presence of both S-bonded and O-bonded DMSO. The two intense CO stretching bands suggested a cis geometry of the two carbonyl ligands and a similar arrangement for the chloride ligands was suggested by the two rather weak Ru−Cl stretching bands. Also the ^{13}C NMR spectrum of **2** (Table 15) was in agreement with a *cis,cis,cis* geometry for the complex. The quality of the microcrystals obtained was not good enough for X-ray investigation but, in agreement with what observed with the other complexes (see above and below), we suggest that the O-bonded DMSO is trans to CO, while the S-bonded DMSO is trans to Cl. Time-driven ^{1}H NMR spectra confirmed that complex **2** evolves in chloroform solution to the isomer **3**.

Complex **3** was obtained in high yield by adopting reaction conditions closely similar to those reported in the literature[6] for the synthesis of the uncharacterized bis(carbonyl) derivative of *cis*-RuCl$_2$(DMSO)$_4$ (refluxing toluene) (eq 3). The main

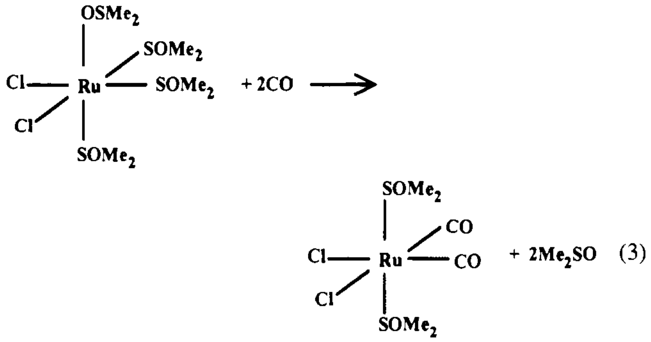

3

Table 16. Selected IR Absorption Bands of Compounds **1**–**6** (cm^{-1})

complex	ν_{CO}	ν_{SO}(DM*S*O)	ν_{SO}(DMS*O*)	ν_{Ru-O}	ν_{Ru-S}	ν_{Ru-Cl}
1	1995 (vs)	1134 (vs)	924 (s)	472 (m)	422 (m)	332, 307 (m)
2	2077, 2020 (vs)	1131 (s)	926 (s)	473 (m)	422 (m)	326, 294 (m)
3	2089, 2035 (vs)	1129 (s)			412 (m)	328, 311 (m)
4	2129 (br), 2060 (vs)		933 (s)	470 (m)		325, 296 (m)
5	1979 (vs)	1116 (vs)	947 (s)	459 (m)	414 (m)	340 (s)
6	2054, 1984 (vs)		951 (s)	470, 460 (m)		331 (s)

Table 17. CO Stretching Frequencies (cm^{-1}) of Compounds **1**–**6** in CHCl$_3$ Solution

complex	frequency	complex	frequency
1	2007	**4**	2134 (br), 2063
2	2083, 2023	**5**	1983
3	2093, 2038	**6**	2067, 1998

structural features of the complex were given by the solid state IR spectrum (Table 16), which also confirmed the presence of exclusively S-bonded DMSO. As in the case of **2**, the presence of two C–O and two Ru–Cl stretching bands suggested a cis geometry for those ligands. Since the ^{1}H NMR spectrum showed a single resonance for DM*S*O, the geometry of **3** could be unambiguously assigned as *cis,trans,cis*-Ru(CO)$_2$(DM*S*O)$_2$Cl$_2$. Single-crystal X-ray investigation confirmed the proposed geometry (Figure 2). As shown by ^{1}H NMR, light-protected chloroform solutions of **3** are indefinitely stable at room temperature. Exposure of **3** to solar or UV light lead to decomposition of the complex or to formation of *trans*-RuCl$_2$(DM*S*O)$_4$ when DMSO was present in solution.

By replacing toluene with a less high boiling but more polar solvent such as ethanol, a tris-carbonylated species (**4**) was obtained upon refluxing *cis*-RuCl$_2$(DMSO)$_4$ under a CO stream (eq 4). Even though the presence in **4** of a single DMS*O* and two cis chloride ligands was deduced by the ^{1}H NMR and IR spectra (Tables 14 and 16), the ^{13}C NMR spectrum (Table 15) did not allow to distinguish between a *fac*- and a *mer,cis*-Ru(CO)$_3$(DMS*O*)Cl$_2$ geometry for the complex, both of them having two equivalent carbonyls. Single-crystal X-ray analysis of **4** (Figure 3) showed that, as expected, the three carbonyl groups are in the thermodynamically favored facial disposition.

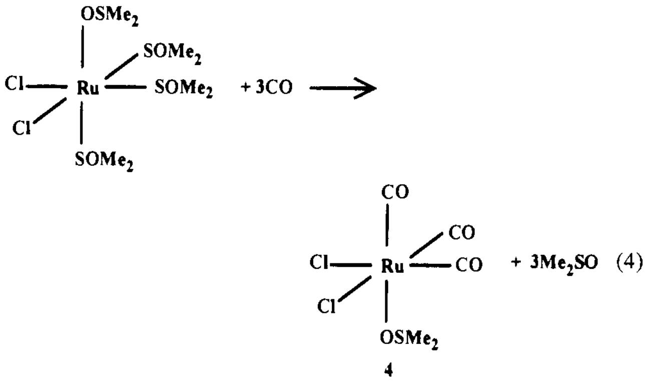

(4)

4

Reactions of *trans*-RuCl$_2$(DMSO)$_4$ with CO. As for the cis isomer, reaction between *trans*-RuCl$_2$(DM*S*O)$_4$ and CO at room temperature and ambient pressure was first monitored by means of ^{1}H NMR spectroscopy in CDCl$_3$. The signal of *trans*-RuCl$_2$(DM*S*O)$_4$ was slowly replaced by two resonances in a 2:1 ratio, one for S-bonded and the other for O-bonded DMSO (Table 14), attributable to a monocarbonyl species **5**. After reaching a maximum concentration in approximately 2 h, complex **5** was slowly replaced by a bis(carbonyl) complex (**6**), characterized by a single resonance for O-bonded DMSO (Table 14) of the same intensity as that of free DMSO. This second step was complete in 12 h. The slow evolution of **6** to **3** was observed for longer reaction times.

As in the case of **1**, the monocarbonyl species **5** was obtained in good yield by running the reaction between *trans*-RuCl$_2$(DM*S*O)$_4$ and CO in methanol (eq 5). Beside the presence of

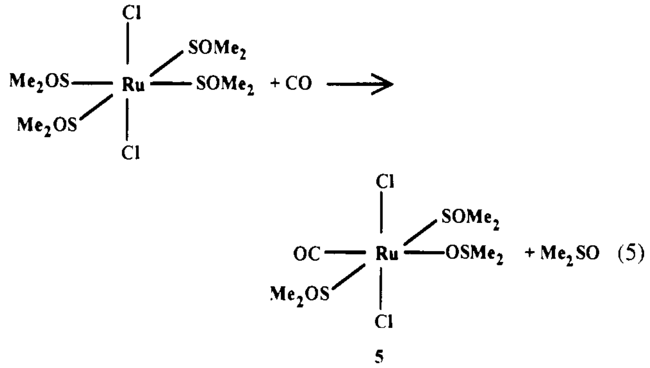

(5)

5

coordinated CO and of both S-bonded and O-bonded DMSO ligands, the solid state IR spectrum of **5** (Table 16) suggested that the two chlorides had preserved a trans geometry as in the precursor. Combined IR and NMR evidence suggested a *trans,trans,trans*-Ru(CO)(DMS*O*)(DM*S*O)$_2$Cl$_2$ geometry for **5**, with the O-bonded DMSO trans to CO. It was confirmed by the single crystal X-ray structure (Figure 4). The geometry of **5** is a further example of how coordination of CO induces the selective S to O isomerization of the DMSO trans to it. Complex **5** was converted almost quantitatively to its isomer **1** upon refluxing in toluene for 1 h.

Isolation of **6** in good yield was obtained under the same conditions of the synthesis of **5**, by simply prolonging the reaction time (eq 6).

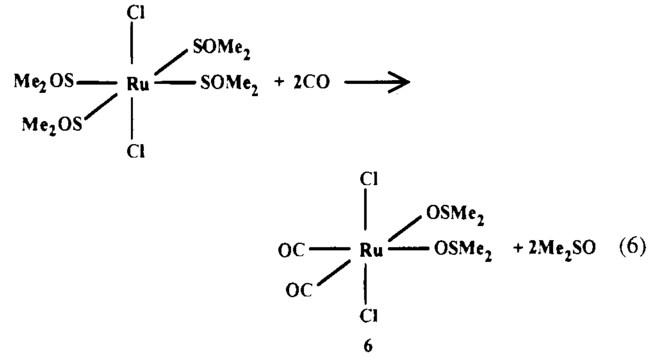

(6)

6

The main structural features of **6**, i.e. the presence of exclusively O-bonded DMSO ligands, a cis geometry of the two carbonyls and a trans geometry of the two chlorides were easily deduced by the solid state IR spectrum (Table 16). The cis geometry of the two DMS*O* ligands was also suggested by the presence of two Ru–O stretching bands. ^{1}H and ^{13}C NMR spectra showed that both the two DMS*O* and the two CO ligands are equivalent to each other. Therefore the geometry of **6** could be unambiguously assigned as being *cis,cis,trans*-Ru(CO)$_2$(DMS*O*)$_2$Cl$_2$. As observed above, in chloroform solution

Table 18. ^{1}H Chemical Shifts of Compounds **7**–**13** in $CDCl_3$ Solution (ppm)

complex	DMSO	Py (Hα)	Py (Hγ)	Py (Hβ)
7	3.55 (s, 3, A[a]), 3.52 (s, 3, A), 3.51 (s, 3, B[a]), 3.33 (s, 3, B)	9.07 (m, 2)	7.82 (m, 1)	7.38 (m, 2)
8	3.50 (s, 3), 2.87 (s, 3)	9.21 (m, 2)	8.02 (m, 1)	7.59 (m, 2)
9	3.52 (s, 6)	8.90 (m, 2)	7.90 (m, 1)	7.45 (m, 2)
10		8.89 (m, 4)	7.88 (m, 2)	7.41 (m, 4)
11		8.96 (m, 2)	8.00 (m, 1)	7.56 (m, 2)
12	3.38 (s, 6)	9.17 (m, 2, A[b]), 8.68 (m, 2, B[b])	7.85 (m, 1, A), 7.76 (m, 1, B)	7.39 (m, 2, A), 7.27 (m, 2, B)

[a] Signals of DMSO A and B were assigned by means of a NOESY spectrum. [b] Signals of py A and B were assigned by means of a COSY spectrum.

Table 19. ^{13}C Chemical Shifts of Compounds **7**–**13** in $CDCl_3$ Solution (ppm)

complex	CO	py	DMSO
7	194.0 (1)	155.8 (2), 138.4 (1), 124.6 (2)	49.0 (1), 48.9 (1), 44.9 (1), 44.6 (1)
8	191.4 (1), 187.4 (1)	153.8 (2), 139.6 (1), 125.9 (2)	50.2 (1), 43.9 (1)
9	188.4 (2)	155.1 (2), 139.1 (1), 125.9 (2)	46.8 (2)
10	194.8 (2)	152.6 (4), 138.7 (2), 125.1 (4)	
11	185.3 (1), 184.7 (2)	153.9 (2), 139.9 (1), 126.2 (2)	
12	200.4 (1)	154.3 (2), 152.9 (2), 138.2 (1), 137.7 (1), 124.6 (2), 124.2 (2)	47.2 (2)

complex **6** is unstable with respect to its isomer **3**, the process being almost complete in 2 days at room temperature according to NMR spectra.

When *trans*-$RuCl_2(DMSO)_4$ was reacted with CO under more drastic conditions, such as refluxing toluene or ethanol, trans to cis isomerization of the two chlorides occurred and the same bis and tris-carbonylated compounds **2**–**4** obtained from *cis*-$RuCl_2(DMSO)_4$ were isolated.

Reactivity of Compounds 1–6 with Nitrogen Ligands. In analogy to what already done with the Ru(II) precursors[12] and with the Ru(III) carbonyls,[9] the reactivity of the carbonylated species **1**–**6** with nitrogen donor ligands was investigated. We focused mainly on pyridine. The reactivity of **2** was not studied because of the difficulties related to its synthesis.

Reaction of **1** with a slight excess of py in refluxing methanol involved the replacement of the O-bonded DMSO with formation of *cis,cis,cis*-$Ru(CO)(py)(DMSO)_2Cl_2$ (**7**) (eq 7).

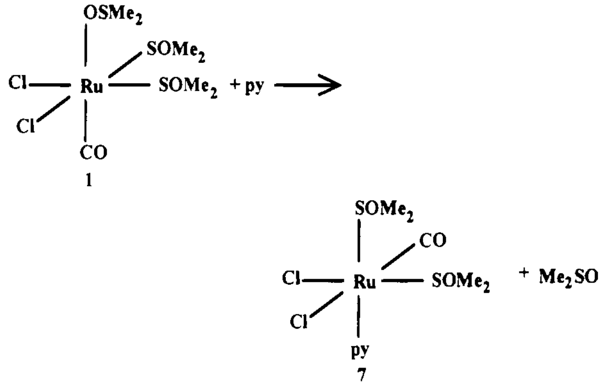

(7)

The all *cis* geometry of **7** was clearly indicated by the four inequivalent DMSO methyl groups in the ^{1}H and ^{13}C NMR spectra of the complex (Tables 18 and 19, respectively). Formation of **7** from **1** involves obviously a geometrical rearrangement of the complex, presumably through the formation of a suitable pentacoordinated intermediate. When the reaction was followed by ^{1}H NMR in deuterated chloroform at room temperature, no intermediate or isomeric product was detected. Two isomers with an all *cis* geometry are possible depending whether CO is trans to Cl or to DMSO. According to what reported above, the second hypothesis is less likely, since a DMSO trans to CO would be expected to be O-bonded. The geometry predicted by NMR data was confirmed by X-ray analysis of **7** (Figure 5). A NOESY experiment allowed the assignment of the methyl groups belonging to the same DMSO through the intraligand NOE connections. The absence of interligand cross-peaks did not allow to establish which DMSO ligand is cis to pyridine.

The reaction of **3** with a stoichiometric amount of py at room temperature was followed through ^{1}H NMR in $CDCl_3$. Replacement of one DMSO was observed, yielding two isomers of formula $Ru(CO)_2(py)(DMSO)Cl_2$ in a 1:5 ratio (eqs 8 and 9).

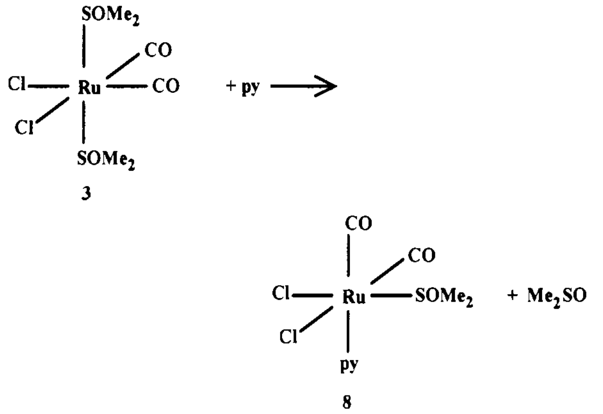

(8)

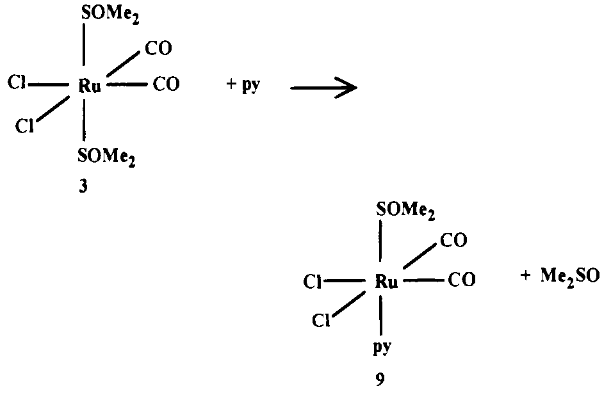

(9)

The minor isomer (**8**) was isolated in high yield by running the reaction in methanol, from where it precipitates due to its low solubility. Combined IR (two carbonyl and two Ru–Cl stretching bands) and ^{1}H NMR evidence (inequivalent DMSO methyl resonances) allowed to assign a *cis,cis,cis*-$Ru(CO)_2(py)$-

(DM*S*O)Cl_2 geometry to **8**. As reported above for **7**, also in **8** the DM*S*O is assumed to be trans to a Cl rather than to a CO. Isomer **9** was isolated from the mother liquor of the synthesis of **8** and, according to spectroscopic evidence, was found to have a *cis,trans,cis*-Ru(CO)$_2$(py)(DM*S*O)Cl_2 geometry. This was also confirmed by the determination of its X-ray crystal structure (Figure 6).

Reaction of **3** with an excess of pyridine in refluxing methanol, led to the isolation of the known disubstituted derivative *cis,cis,trans*-Ru(CO)$_2$(py)$_2$Cl$_2$ (**10**) (eq 10).[15]

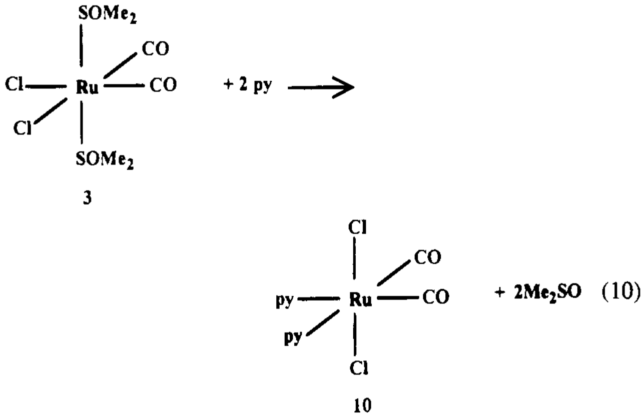

3 10 (10)

The cis to trans isomerization of the chloride ligands was clearly indicated by the single strong Ru−Cl stretching band in the IR spectrum of **10**. The same complex was also obtained upon reaction of **6** with pyridine at room temperature (see below).

The reactivity of **4** with pyridine followed the expected path, involving the selective replacement of the weakly bonded DMS*O* to give *fac*-Ru(CO)$_3$(py)Cl$_2$ (**11**) (eq 11).

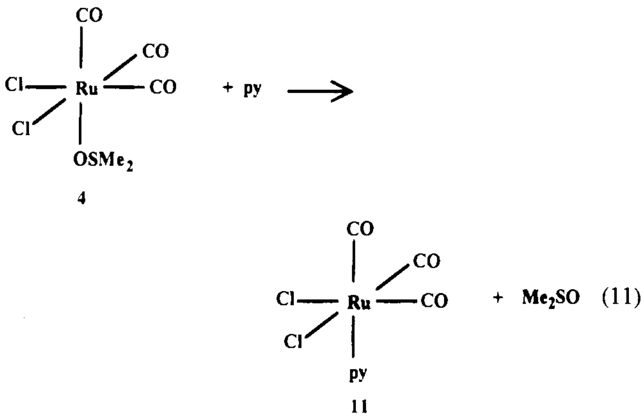

4 11 (11)

The same complex had been previously obtained by reaction of [Ru(CO)$_3$Cl$_2$]$_2$ dimer with pyridine at room temperature.[15]

The reaction of both **5** and **6** with a slight excess of pyridine at room temperature involved replacement of the weakly bonded DMS*O* ligands and, in the case of **5**, also of one of the two trans S-bonded DMSOs. As shown by IR spectroscopy, in both cases the trans geometry of the chloride ligands was retained, yielding *cis,cis,trans*-Ru(CO)(DM*S*O)(py)$_2$Cl$_2$ (**12**) and *cis,cis,trans*-Ru(CO)$_2$(py)$_2$Cl$_2$ (**10**), respectively (eqs 12 and 13).

The signals of the two inequivalent pyridines in **12** were distinguished by means of a COSY spectrum. Interestingly enough, NMR evidence shows that in the reaction of **5** with pyridine, replacement of one of the two trans DM*S*O ligands occurs first, followed by the slower substitution of the DMS*O* trans to CO.

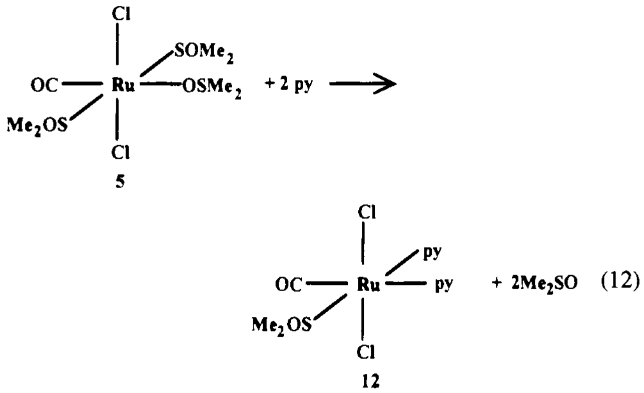

5 12 (12)

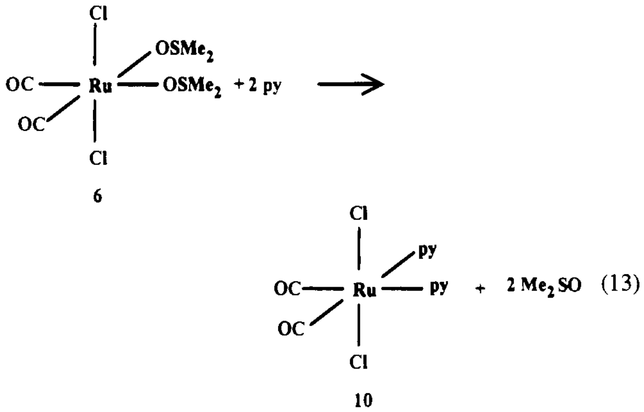

6 10 (13)

Structural Comments. Too few data are so far available to draw definitive conclusions about the mutual structural influence of carbonyl and sulfoxide ligands. In any case, it is interesting to observe that the Ru−S bond distances in *cis,trans,cis*-Ru(CO)$_2$(DM*S*O)$_2$Cl$_2$, **3**, (average 2.358(5) Å) lie among the longest values found in *trans*-Ru(DM*S*O)$_2$ fragments (average 2.330(4) Å). It seems likely that this is attributable to the electron-withdrawing ability of the carbonyl groups, which further reduce the π-back-bonding in the Ru−S bonds. As expected, substitution of one DM*S*O with a pyridine, which changes the complex from **3** to **9**, shortens the Ru−S bond distance from 2.358(5) to 2.322(7) Å.

Furthermore, it is worth of note that the average Ru−Cl bond length, trans to CO (**3**, **4**, **7**, **9**), of 2.406(5) Å is slightly shorter than that of 2.426(3) Å, trans to DM*S*O (**1**), suggesting that the latter exerts a slightly larger σ trans influence.

Finally, we can observe that the Ru−C bond distances in the six structurally characterized compounds show a general increase by increasing the number of coordinated carbonyls, going from 1.815(7), 1.839(4), and 1.859(3) Å in the monocarbonyl derivatives **5**, **1**, and **7**, respectively, to 1.87(1) and 1.886(2) Å in the biscarbonyl compounds **9** and **3**, up to 1.898(16) Å in the tris(carbonyl) complex **4**. This trend is attributable to a decrease of the π-back-bonding from Ru(II) to CO π^* orbitals due to the increased competition. As a matter of fact, the CO stretching frequencies increase in the above order from 1979 cm^{-1} in **5**, to 2060, 2129 cm^{-1} in **4**. The average C−O bond lengths are, on the overall, in agreement with this trend, decreasing from 1.15(1) Å in **5**, to 1.12(1) Å in **4**. A particularly short value (1.119(3) Å) is observed for *cis,cis,cis*-RuCl$_2$(DM*S*O)$_2$(CO)(py), **7**. It is interesting to note that in this complex, the Ru−C bond distance of 1.859(3) Å is the longest among the three monocarbonyl compounds. This would suggest

---

[15] Benedetti, E.; Braca, G.; Sbrana, G.; Salvetti, F.; Grassi, B. *J. Organomet. Chem.* **1972**, *37*, 361.

Scheme 1. Reactions of *cis*-RuCl$_2$(DMSO)$_4$ with Carbon Monoxide at Ambient Pressure

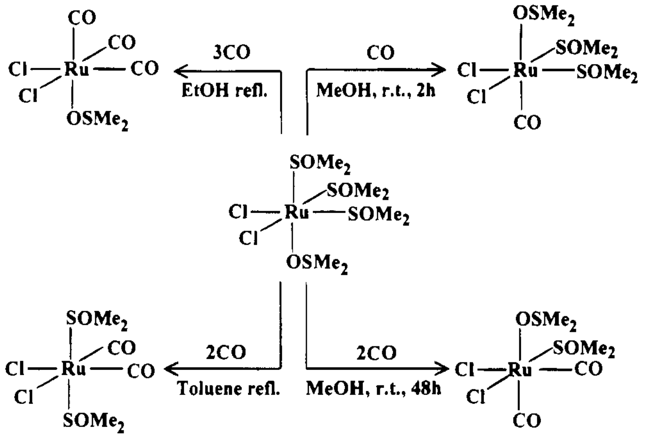

Scheme 2. Reactions of *trans*-RuCl$_2$(DMS*O*)$_4$ with Carbon Monoxide at Ambient Pressure

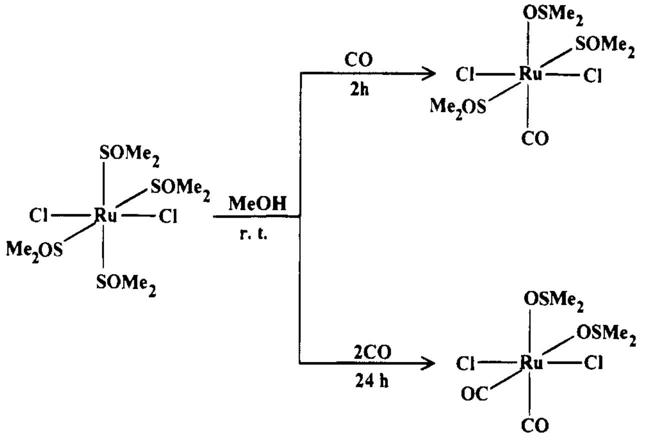

a further weakening of the Ru−C π bonding, by means of the pyridine molecule.

Discussion

The reactivity of *cis* and *trans*-RuCl$_2$(DMS*O*)$_4$ with carbon monoxide is summarized in Schemes 1 and 2, respectively. The common feature of this series of chloride−DMSO−carbonyl compounds (with the exception of **3**) is that coordination of CO always induces a selective S to O linkage isomerization of the DMSO trans to it. As already observed with Ru(III) species,[9] this linkage isomerization can be attributed exclusively to electronic reasons, since it avoids competitions for π-back-bonding electrons between CO and the weaker π-acceptor DMS*O*.

The geometry of the products **1**−**6** can be suitably compared to that of similar compounds bearing another ligand, (L = P, N, As, S donor) instead of DMSO. Most of the known complexes of formula Ru(CO)L$_3$X$_2$ have either a *mer,cis* or a *mer,trans* geometry; the thermodynamically stable form is the *mer,cis* isomer.[1,5] The *fac* geometry has been forced by using tridentate ligands.[16,17] We reported here two examples of monocarbonyl species, one with a *mer,trans* geometry (**5**) and the other with a *fac* geometry (**1**). We have also shown that **1** is thermodynamically more stable than **5**. This is apparently the first case where a stable *fac* geometry is obtained with monodentate L ligands. The preference for a facial arrangement in the case of DMSO can be attributed to the π-back-bonding ability of this ligand when S-bonded, which disfavors coordination of two DMS*O* ligands trans to each other. It should be noted, however, that S-bonded and O-bonded DMSO behave quite differently both from an electronic and a steric point of view and it is therefore questionable whether they should be considered as being "the same ligand".

The complexes of stoichiometry Ru(CO)$_2$L$_2$X$_2$ are by far the most numerous in the literature.[1] Of the four possible geometrical isomers, *cis,trans,cis*, *cis,cis,trans*, *cis,cis,cis* and *trans,trans,trans* (there has been no confirmed report of any *trans,cis,cis*-Ru(CO)$_2$L$_2$X$_2$), the *cis,cis,trans* isomer appears to be the most stable for amine adducts, while for phosphine, arsine and sulphide derivatives the thermodynamically preferred product is the *cis,trans,cis* isomer.[1] This was found true also for the DMSO derivatives, where both *cis,cis,cis*-Ru(CO)$_2$(DMS*O*)(DMS*O*)Cl$_2$ (**2**) and *cis,cis,trans*-Ru(CO)$_2$(DMS*O*)$_2$Cl$_2$ (**6**) thermally isomerize to *cis,trans,cis*-Ru(CO)$_2$(DMS*O*)$_2$Cl$_2$ (**3**). The mechanisms proposed for the various rearrangements of the complexes Ru(CO)$_2$(L)$_2$Cl$_2$ (L = phospine) all involve the dissociation of a carbonyl ligand as a key step.[4] With DMSO compounds, on the contrary, the key step is very likely dissociation of DMSO, as suggested by the small signal of free DMSO observed by NMR during the isomerization. This is also in agreement with the further reactivity of this complexes, which never involved CO loss (see below).

We had no spectroscopic evidence of a *trans,trans,trans* derivative. The attempts to generate it by photochemical isomerization of the thermodynamically most stable isomer, as reported for the corresponding phosphine adducts,[4] led to decomposition products or, in the presence of free DMSO, to *trans*-RuCl$_2$(DMS*O*)$_4$.

Complexes of stoichiometry Ru(CO)$_3$LX$_2$ are the least numerous, being more difficult to synthesize; all the known compounds have a facial geometry.[1] The DMSO complex **4** is no exception to this rule, since this geometry is obviuosly dictated by the three carbonyl ligands which prefer a facial arrangement. However, the facile preparation of the complex and the ease of substitution of the remaining DMSO, make **4** a suitable and convenient precursor for other tris(carbonyl) species.

Reaction of compounds **1**−**6** with a neutral ligand such as pyridine leads to the substitution of DMSO. The number of DMSO ligands replaced and the geometry of the resulting complexes depend on the reaction conditions. In no case was replacement of CO observed. In this respect, the bis(carbonyl) complexes **3** and **6** behave quite differently from their phosphine counterparts, whose reactivity has been detailedly studied by Mawby and co-workers.[4] For example, Ru(CO)$_2$(PMe$_2$Ph)$_2$Cl$_2$ isomers react with a wide variety of L ligands to give monosubstituted products Ru(CO)(PMe$_2$Ph)$_2$(L)Cl$_2$. Ru−CO bond cleavage can be induced either by the action of heat or of light. The reactivity of **5** and **6** is straightforward at room temperature and recalls that of the precursor *trans*-RuCl$_2$(DMS*O*)$_4$: two pyridines are coordinated in cis position while the trans arrangement of the two chloride ligands is maintained. A similar straightforward behavior is observed with **4**. On the other hand, reaction of **1** and **3** with py is more complicated since can lead to geometrical isomerization.

Conclusions

In this paper we report the synthesis and structral characterization of a series of new chloride-carbonyl compounds of Ru(II) with DMSO of formula Ru(CO)$_x$(DMSO)$_{4-x}$Cl$_2$ ($x = 1-3$). Even though similar complexes with ligands other than DMSO

---

[16] Chatt, J.; Leigh, G. J.; Storace, A. P. *J. Chem. Soc. A* **1971**, 1380.
[17] Siegl, W. O.; Lapporte, S. J.; Collman, J. P. *Inorg. Chem.* **1973**, *12*, 674.

are well known, this is the first example of well-characterized compounds of this type. Among the two monocarbonyl compounds, **1** and **5**, complex **1** represents a rare example of $Ru(CO)L_3Cl_2$ species with a *fac* arrangement of the monodentate L ligands. Three bis(carbonyl) species have been isolated, **2**, **3** and **6**, the thermodynamically most stable one being that with a *cis,trans,cis* geometry. The only tris(carbonyl) complex, **4**, has the expected *fac* arrangement of the three carbonyl ligands. The selective S to O linkage isomerization induced by coordination of CO on the trans sulfoxide has been attributed to electronic reasons.

The reactivity of compounds **1**–**6** with a neutral ligand such as pyridine has been also investigated, and several derivatives were isolated and characterized. Remarkably, unlike with the corresponding phosphine complexes, replacement of carbon monoxide was never observed, all the products **7**–**12** deriving from **1**–**6** upon replacement of DMSO ligands. This feature makes compounds **1**–**6** particularly interesting and versatile precursors in the synthesis of Ru(II)–carbonyl species.

Finally, the antitumor properties of *cis*- and *trans*-$RuCl_2(DMSO)_4$[10,18] and their patterns of interaction with nitrogen bases of DNA are well established.[19] The greater lability of DMSO ligands compared to CO observed in **1**–**6**, suggests that the new carbonyl complexes might be used as suitable sources of ruthenium fragments of defined geometry. Their chemical behavior in aqueous solution and their *in vitro* interactions with DNA will be accordingly investigated.

Acknowledgment. This work was supported by the Italian Ministry for University and Scientific and Technological Research (40% grant). A generous loan of hydrated $RuCl_3$ from Johnson Matthey PLC is gratefully acknowledged. Thanks are due to the Institute of Mineralogy and Petrografy of the University of Trieste for data collection on the KUMA KM-4 diffractometer.

Supporting Information Available: Lists of anisotropic thermal parameters and H-atom parameters (12 pages). Ordering information is given on any current masthead page.

IC9414637

---

(18) Mestroni, G.; Alessio, E.; Sava, G.; Pacor, S.; Coluccia, M. In *Metal Complexes in Cancer Chemotherapy*; Keppler, B. K., Ed.; VCH Verlag: Weinheim, Germany, 1993; p 159.

(19) Coluccia, M.; Sava, G.; Loseto, F.; Nassi, A.; Boccarelli, A.; Giordano, D.; Alessio, E.; Mestroni, G. *Eur. J. Cancer* **1993**, *29A*, 1873.